POLITEKNIK NEGERI BALI

matriX

JURNAL MANAJEMEN TEKNOLOGI DAN INFORMATIKA

Vol. 15 No. 1 | Page 1- 49 | March 2025 | ISSN 2580-5630

Editors

Reviewers

PREFACE

We would like to present, with great pleasure, the first issue of Matrix: Jurnal Manajemen Teknologi dan Informatika in Volume 15, 2025. This journal is under the management of Scientific Publication, Research and Community Service Center, Politeknik Negeri Bali, and is devoted to covering the field of technology and informatics management including managing the rapid changes in information technology, emerging advances in electrical and electronics and new applications, implications of digital convergence and growth of electronics technology, and project management in electrical, mechanical or civil engineering. We would also like to express our deepest appreciation and gratitude for the dedication and contribution of Mrs. Gusti Nyoman Ayu Sukerti, S.S., M.Hum as the previous Editor-in-Chief, who has led and oversaw the development of this journal during her leadership. We would like to inform you that the publication of this first edition has been delayed due to the Editor-in-Chief transition process in early 2025. Nevertheless, we remain committed to maintaining the quality and accuracy of the editorial process. The scientific articles published in this edition were written by researchers from Universitas Pendidikan Nasional, Politeknik Elektronika Negeri Surabaya, Universitas Semarang, Universitas Logistik dan Bisnis Internasional, and ITB STIKOM Bali. Articles in this issue cover topics in the field of Analysis of Financial Feasibility Installing Parking Meters in Gianyar Regency (Case Study: Jalan Ngurah Rai – Gianyar), Data Acquisition of Flow Sensor Based to Measure Water Flow in Underground Drainage, Analysis of Corn Production in Indonesia Using Business Intelligence Technology Based on Power BI, Development of A Hybrid Model for Website Functional Evaluation Based on ISO/IEC 25010 and SERVQUAL, Lightweight CNN with Wavelet-Attention for Fingerprint Liveness Detection. Finally, we would like to thank the reviewers for their efforts and hard work in conducting a series of review phases thoroughly based on their expertise. We hope that the work of the authors in this issue will be a valuable resource for other researchers and will stimulate further research into the vibrant area of technology and information management in specific, and engineering in general.

Politeknik Negeri Bali, 31 March 2025

Editor-in-chief

Dewa Ayu Indah Cahya Dewi, S.TI., M.T.

ISSN: 2580-5630

Table of contents

Matrix: Jurnal Manajemen Teknologi dan Informatika
Volume 15 Issue 1 Year 2025 Pages 1-8
DOI: http://dx.doi.org/10.31940/matrix.v15i1.1-8
URL: http://ojs2.pnb.ac.id/index.php/matrix

Analysis of financial feasibility installing parking meters in Gianyar Regency (case study: Jalan Ngurah Rai – Gianyar)

I Gede Fery Surya Tapa [1]*, I Nyoman Indra Kumara [2], Decky Cipta Indrashwara [3], I Ketut Sutapa [4], I Nengah Darma Susila [5]

[1, 2, 3] *Department of Civil Engineering, Universitas Pendidikan Nasional, Indonesia*
[4] *Civil Engineering Department, Politeknik Negeri Bali, Indonesia*
[5] *Mechanical Engineering Department, Politeknik Negeri Bali, Indonesia*

*Corresponding Author: *ferysuryatapa@undiknas.ac.id*

Abstract: The increase in the number of motorized vehicles in Gianyar Regency has an impact on parking needs, as is the case on Jalan Ngurah Rai, Gianyar Regency. The data used in this research includes primary data obtained through parking inventory surveys, parking patrol surveys, and secondary data in the form of parking PD income data, parking meter price data, obtained from the Gianyar Regency Transportation Service. Parking characteristics for motorcycles are: parking inventory 95 SRP, parking volume in the 14-hour survey was 2147 vehicles, parking duration was 0.9318 hours, the parking capacity is 102 vehicles/hour, the parking provision is 1356 vehicles, and the parking index is 1,148. Parking characteristics for light vehicles are: parking inventory 88 SRP, parking volume in the 14-hour survey was 837 vehicles, parking duration was 1.0182 hours, the parking capacity is 85 vehicles/hour, the parking provision is 1128 vehicles, and the parking index is 0.92. The financial feasibility analysis for scenario 1 (fixed rate LV= 2000/one parking, MC= 1000/one parking) it is obtained that NPV = 3,153,280,747 > 0, BCR = 1,634 > 1, and IRR = 51% > MARR= 20%. For scenario 2 (fixed parking rate, LV=3000/hour, MC= 2000/hour) we get NPV = 8,998,418,237 > 0, BCR = 2,810 > 1, and IRR = 136%> MARR= 20%. For scenario 3 (fixed parking rate, first hour LV= 3000, MC= 2000, 1 hour later increase in LV= 2000/hour, MC= 1000/hour) obtained NPV = 11,625,402,449 > 0, BCR= 3,338 > 1, and IRR= 174%> MARR= 20%.

Keywords: financial feasibility, parking characteristics, parking meters

History Article: Submitted 31 July 2024 | Revised 11 November 2024 | Accepted 21 March 2025

How to Cite: I. G. F. S. Tapa, I. N. I. Kumara, D. C. Indrashwara, I. K. Sutapa, and I. N. D. Susila, "Analysis of financial feasibility installing parking meters in Gianyar Regency (case study: Jalan Ngurah Rai – Gianyar)", *Matrix : Jurnal Manajemen Teknologi dan Informatika*, vol. 15, no. 1, pp. 1–8, 2025. doi.org/10.31940/matrix.v15i1.1-8.

Introduction

Currently, most parking payment systems are still carried out conventionally. Conventional parking payments are made by paying the parking attendant using a ticket [1]. Income from the parking sector contributes to Regional Original Income (PAD), but there is a leak in the conventional system and will affecting Regional Original Income [2]. On the other hand, one of the causes. The high number of leaks that occur is due to an unorganized parking system [3]. New policies regarding more efficient parking management solutions need to be implemented, one of them is by implementing an Electronic Parking Terminal (TPE) system [4].

With the development of technology, parking problems can be overcome with the use of the Electronic Parking Terminal [5]. Use of Parking Terminal Electronics must be carried out based on local regional regulations for determine which roads or areas the Parking Terminal will be implemented on Electronic [6]. In regional regulations must also be formulated the amount of fines for violations of parking provisions [7]. Key to success the use of Electronic Parking Terminals is a law enforcement application strict against parking violations [8]. In Indonesia, electronic parking terminals already exist used in roadside parking areas in Jakarta, Bandung, Bali and Palembang [9].

Jalan Ngurah Rai in Gianyar Regency is very close to the center Shopping [10]. The many shops on Jalan Ngurah Rai create attraction travel that affects parking on Jalan Ngurah Rai [11].

Jalan Ngurah Rai is one of the roads with the highest parking revenue in the City Gianyar, so there is potential for implementing an Electronic Parking Terminal [12].

To overcome this parking problem as a first step is needed there is a study regarding parking [13]. Therefore, a study is needed regarding Analysis of Parking Characteristics and Financial Feasibility of Implementation Electronic Parking Terminal on Jalan Ngurah Rai, Gianyar Regency.

Methodology

The research steps were carried out in stages including preliminary studies, identification of problems and determination of research objectives, literature study, data collection including primary data including: parking inventory survey data on the number of parking facilities available [14]. Parking spaces with a standard SRP size of 2.5 x 5 m for light vehicles and 0.75 x 2 m for motorcycles and parking patrol surveys can obtain data regarding parking characteristics, including: number of parked vehicles (parking volume), parking accumulation, and vehicle parking time, and secondary data includes: Data Parking rates are obtained from the Gianyar Regency Regional Government [15]. Prices for parking meters are obtained from the Gianyar Regency Transportation Service. The cost of installing CCTV cameras was obtained from installation data by the Gianyar Regency Transportation Service in 2018. The 2018 Gianyar Regency UMK level was used to determine the salary of parking attendants, with a 2 shift system. Inflation rate for the last 7 years from BPS [16]. The growth rate of the population aged 17-75 years obtained from BPS is used to predict the increase in vehicle parking volume. The loan interest rate is obtained from the reference interest rate from Bank Indonesia. Parking meter network system in Gianyar Regency. The applicable Tabanan Regency Parking Rates are in accordance with the Gianyar Regency Regional Regulations.

Results and Discussions

Parking Characteristics Analysis

The existing parking system on Jalan Ngurah Rai-Gianyar is a roadside parking system. Parking spaces on Jalan Ngurah Rai-Gianyar are divided into parking spaces for motorcycles and light vehicles. The results of the parking inventory survey can be seen in Table 1.

Table 1. Parking inventory on Jalan Ngurah Rai-Gianyar

No	Type of Vehicle	Length (m)	Parking Angle Degree (°)	Plot Size (m^2)	Plot Estimate
1	Light Vehicles	35	90	-	14
2	Light Vehicles	185	45	-	74
3	Motorcycles	71.25	45	-	95

Based on Table 1 the number of parking lots on Jalan Ngurah Rai - Gianyar is obtained from the number of light vehicles when the special light vehicle parking space is fully filled, namely 14 SRP in length 35 m road with a parking angle of 90 degree, and for a parking angle of 45 degree as much as 74 SRP with a road length of 185 m. The number of motorcycles parking lots is 95 with a road length of 71.25 m with a parking angle of 45 degree. In this parking space there are no lines/markings for parking spaces for motorcycles, therefore the number of parking lots is obtained when the parking space is fully occupied by parked vehicles.

Parking Volume

From the survey results, it can be seen that the total volume of vehicles parked during the 10 hours of observation of the Jalan Ngurah Rai - Gianyar section is as shown in Table 2.

Table 2. Volume of parked vehicles

No	Type of Vehicle	Total Vehicle Volume during the Survey (vehicles)	Average Volume (vehicles/hour)
1	Light Vehicles	837	59
2	Motorcycles	2147	153

From Table 2 it can be seen that the total volume of light vehicles parked on the Jalan Ngurah Rai - Gianyar section is 837 vehicles with the average vehicle parked every hour being 59 vehicles/hour. Meanwhile, the total volume of motorcycles parked is 2147 vehicles with the average vehicle parked every hour being 153 vehicles/hour.

Parking Accumulation

From the survey results, it can be seen the accumulation of vehicles parked every 1 hour. The highest accumulation at each survey time can be seen in Table 3.

Table 3. Parking accumulation

No	Type of Vehicle	Times (hours)	Accumulation (vehicles/hour)
1	Light Vehicles	13.00 – 14.00	78
2	Motorcycles	19.00 – 20.00	117

Table 3 can be seen that the highest accumulation on Jalan Ngurah Rai - Gianyar for light vehicles at 13.00 – 14.00 WITA is 78 vehicles. The highest accumulation of motorcycles occurred at 19.00 – 20.00 WITA amounting to 117 vehicles.

Parking Duration

From the results of the survey that has been carried out, the average parking time can be analyzed. Average Parking Time can be seen in Table 4.

Table 4. Parking duration

No	Type of Vehicle	Average Parking Duration (hours)
1	Light Vehicles	1.0376
2	Motorcycles	0.9318

Based on Table 4, the average parking duration during the 14 hours survey period was 0.9318 hours for motorcycles and 1.0376 hours for light vehicles.

Parking Time Distribution

The distribution of parking time for light vehicles on Jalan Ngurah Rai - Gianyar is determined by the largest percentage for the duration parking for 0 – 1 hour is 77.4% and motorcycles for 0 – 1 hour namely 85.7%.

Table 5. Parking time distribution

Parking Time (hours)	Parking Time Distribution	
	Light Vehicles	Motorcycles
1	77.4	85.70
2	15.89	6.80
3	2.63	2
4	0.84	1.35
5	0.60	1.07
6	0.60	0.88
7	0.36	0.28
8	0.12	0.37
9	0.12	0.14
10	0.12	0.23
11	0.36	0.28
12	0.6	0.28
13	0.12	0.23
14	0.24	0.37

From Table 5, it can be seen that vehicles parked on Jalan Ngurah Rai - Gianyar are parked within a period of 14 hours.

Parking Turnover

From the survey results, the parking turnover rate can be found using the Parking Turnover Rate formula. In Table 6 are the results of calculating the parking turnover rate.

Table 6. Parking turnover

Type of Vehicle	Number of Vehicles (Nt)	Number of Plots (S)	Survey Time (T)	Parking Turnover Rate (TR=Nt/(S*T))
	vehicles	vehicles	hours	hours
Light Vehicles	837	88	14	0.672
Motorcycles	2147	95	14	1.614

From Table 6 it can be seen that the level of parking turnover on the road section Ngurah Rai-Gianyar for light vehicles is 0.672 hours and the motorcycles parking turnover rate is 1.614 hours, which means that every hour 1 (one) plot serves more than 1 (one) vehicle.

Parking Capacity

From the survey and data analysis, the parking capacity at the survey location was obtained as shown in Table 7.

Table 7. Parking capacity

Type of Vehicle	Number of Plots (S)	Average Parking Duration (D)	Parking Capacity (KP=S/D)
	vehicles	hours	vehicles/hours
Light Vehicles	88	1.0376	85
Motorcycles	95	0.9318	102

From Table 7 above you can see the parking capacity on Jalan Ngurah Rai - Gianyar can accommodate 85 vehicles/hour for light vehicles and 102 vehicles/hour for motorcycles.

Parking Supply

From Table 8 you can see the results of the analysis of the amount of parking space provision during the 10 hour survey.

Table 8. Parking supply

Type of Vehicle	Survey Time (T)	Average Parking Time (D)	Number of Plots (S)	Insuffiency Factor (f)	Parking Supply Ps = (S*T*f) / D
	hours	hours	vehicles		vehicles
Light Vehicles	14	1.0376	88	0.95	1,128
Motorcycles	14	0.9318	95	0.95	1,356

From Table 8 it can be seen that the parking supply on Jalan Ngurah Rai - Gianyar during the 14 hours survey for light vehicles was 1,128 vehicles and motorcycles amounting to 1,356 vehicles.

Parking Index

The following is the highest parking index for motorcycles and light vehicles in Table 9.

Table 9. Parking index

Type of Vehicle	Times	Parking Accumulation	Parking Capacity	Parking Index
Light Vehicles	13.00-14.00	78	85	0.920
Motorcycles	19.00-20.00	117	102	1.148

From Table 9 above, it can be seen that parking conditions based on peak accumulation on Jalan Ngurah Rai - Gianyar for motorcycles have a parking index of more than 1 (one). This shows that the need for parking spaces at peak conditions exceeds the existing parking capacity. So parking capacity cannot accommodate parking demand during peak hours. Meanwhile, light vehicles have a parking index of less than 1 (one). This shows that there is no need for parking spaces at peak conditions exceeds existing parking capacity. So the parking capacity can accommodate parking demand during peak hours.

Parking Revenue

Revenue is obtained by multiplying the parking fee by the volume of vehicles parked in a certain time period. Created 3 parking rate scenarios that will be used in installing parking meters.

1 Alternative 1 obtains an average annual parking income of IDR 1,092,733,755.-
2 Alternative 2 obtains an average annual parking income of IDR 1,878,488,872.-
3 Alternative 3 obtains an average annual parking income of IDR 2,256,742,579.-

Investment Costs

The costs incurred in installing parking meters are classified into three, namely Initial Investment Costs with a Sub Total of IDR 952,058,920, Operational Costs with a Sub Total of IDR 505,120,000, and Maintenance Costs with a Sub Total of IDR 160,799,928.

Financial Feasibility Analysis

Financial feasibility analysis is carried out with the aim of evaluating financial feasibility. The methods used are NPV, BCR, and IRR. The results of the financial feasibility analysis can be seen in Table 10.

To find NPV, BCR, and IRR, use the equation:

$$BCR = \frac{PWB}{PWC} \quad (1)$$

$$NPV = PWB - PWC \quad (2)$$

IRR is determined by comparing the IRR value with MARR. In this study, the MARR value was determined at 20% per year. For MARR. In this study, the MARR value was determined at 20% per year. For to calculate the IRR value using the try method to calculate the IRR value using the Try and error method.

Table 10. Financial feasibility of all three alternatives

	Alternative 1	**Alternative 2**	**Alternative 3**
NPV	Rp 3,153,280,747	Rp 8,998,418,237	Rp 11,625,402,449
BCR	1.634	2.81	3.34
IRR	51%	136%	174%

Payback Period Method

All alternatives get decent analysis results. So for alternative 1 the payback period is 2 years in 2021, for alternative 2 the payback period is 1 year in 2020, and alternative 3 the payback period is less than 1 year in 2020. This means in those years there has been a return on investment capital.

Sensitivity Analysis

Sensitivity analysis on the installation of parking meters on Jalan Ngurah Rai-Gianyar was carried out by analyzing the sensitivity of benefits and costs, with three (3) sensitivity scenarios, namely: (1) With fixed benefits and increasing costs. (2) With decreasing benefits and increasing costs. (3) With decreasing benefits and increasing costs. Based on the sensitivity analysis calculations that have been carried out, the sensitivity analysis results are obtained in Table 11.

Table 11. Sensitivity analysis of the three scenarios

Scenario	Description	
	Benefit	**Cost**
1	Still	Go on 38%
	Down 29%	Still
	Down 16%	Go on 16%
2	Still	Go on 140%
	Down 58%	Still
	Down 41%	Go on 41%
3	Still	Go on 180%
	Down 65%	Still
	Down 48%	Go on 48%

Conclusion

From the results of calculations and analysis it can be concluded as follows: Parking Characteristics; For light vehicles, the total number of stalls obtained was 14 vehicles at an angle of 90 degrees, and 74 vehicles at an angle of 45 degrees, the parking volume during the 10 hour survey was 837 vehicles, the average accumulation of parking was 78 vehicles/hour, the duration of parking was 1.036 hours, parking turnover of 0.672 hours, parking capacity of 85 vehicles/hour, parking supply of 1128 vehicles, and parking index of 1.148. For motorcycles, the total number of stalls was found to be 95 vehicles at an angle of 45 degrees, the parking volume during the 10 hours survey obtained a parking volume of 153 vehicles, the average accumulated parking was 117 vehicles/hour, the parking duration was 0.9318 hours, parking turnover was 1.614 hours, parking capacity was 102 vehicles/hour, parking supply was 1356 vehicles, and the parking index was 0.920. Financial Feasibility of installing parking meters; Of the three parking rate alternatives that have been analyzed, the three parking rate alternatives meet the requirements for investment worth implementing, namely NPV > 0, BCR > 1, and IRR > interest rate. For the payback period, the payback period for scenario 1 is 2 years in 2021, for scenario 2 the payback period is 1 year in 2020, and for scenario 3 the payback period is less than 1 year in 2020. Sensitivity Analysis: Based on the sensitivity analysis calculations that have been carried out, the following sensitivity analysis results are obtained; For the sensitivity of scenario 1, with investment costs rising up to 38% and fixed income the investment is categorized as not feasible. Thus, with income decreasing by 29% and investment costs remaining the same, and with income decreasing by 16% and investment costs increasing by 16%, the investment is categorized as not feasible. This is because NPV < 1, BCR < 0, and IRR < interest rate. For the sensitivity of scenario 2, with investment costs rising up to 140% and fixed income the investment is categorized as not feasible. Thus, with income decreasing by 58% and investment costs remaining the same, and with income decreasing by 41% and investment costs increasing by 41%, the investment is categorized as not feasible. This is because NPV < 1, BCR < 0, and IRR < interest rate. For the sensitivity of scenario 3, with investment costs rising up to 180% and fixed income the investment is categorized as not feasible. Thus, with income decreasing by 65% and investment costs remaining the same, and with income decreasing by 48% and investment costs increasing by 48%, the investment is categorized as not feasible. This is because NPV < 1, BCR < 0, and IRR < interest rate.

Acknowledgments

First of all, allow the author to express his thanks to Ida Sang Hyang Widhi Wasa/God Almighty because of His generous support, this research can be completed. May Ida Sang Hyang Widhi Wasa/God Almighty always bestow His grace on all parties who have helped carry out and complete this research, as well as on the author and his family.

References

[1] S. Warpani, *Perencanaan Sistem Transportasi*. Bandung: Institut Teknologi Bandung, 1990.

[2] O. Z. Tamin, *Perencanaan dan Pemodelan Transportasi*. Bandung: Institut Tekonologi Bandung, 2000.

[3] M. Giatman, *Teknik Ekonomi*. Jakarta: Jakarta: PT. Raja Grafindo Persada, 2006.

[4] N. W. Negara, I. M. A. Ariawan, and K. D. Nursanjaya, "Kelayakan Finansial Pemasangan Meter Parkir untuk Parkir On Street di Kota Denpasar (Studi Kasus: Jalan Maluku)," *J. Ilm. Tek. Sipil*, vol. 22, no. 1, pp. 1–6, 2018.

[5] I. Soeharto, *Manajemen Proyek (Dari Konseptual ke Operasional)*. Jakarta: Erlangga, 1997.

[6] J. . Oppenlander, *Manual Kajian Rekayasa Lalu Lintas.* Washington, DC: Institut Insinyur Transportasi, 1976.

[7] K. D. Nursanjaya, "Analisis Kelayakan Finansial Penerapan Terminal Parkir Elektronik pada Jalan di Kota Denpasar (On Street Parking) (Studi Kasus: Jalan Maluku Denpasar)," Universitas Udayana, 2017.

[8] I. G. F. . Tapa, I. N. . Kumara, I. . Sutapa, and I. K. . Wijaya, "Analisis Kelayakan Finansial Pengoperasian Bus Trans Metro Dewata di Provinsi Bali," *J. Ilm. Poli Rekayasa*, vol. 18, no. 1, pp. 7–14, 2022.

[9] Y. Dewantari, "Karakteristik dan Analisis Keuangan Parkir On Street (Studi Kasus: Jalan Sumatra Denpasar)," Universitas Udayana, 2017.

[10] LPKM-ITB, *Modul Pelatihan Studi Kelayakan Proyek Transportasi (Lembaga Pengabdian Kepada Masyarakat ITB bekerjasama dengan Kelompok Keahlian Teknik Transportasi, Jurusan Teknik Sipil ITB)*. Bandung: LPKM-ITB, 1997.

[11] I. G. F. . Tapa, I. N. . Kumara, D. . Indrashwara, and I. M. P. . Putra, "Analisis Kelayakan Finansial Terminal Parkir Elektronik Di Kota Tabanan (Studi Kasus: Jalan Gajah Mada Barat)," *J. Darma Agung*, vol. 32, no. 3, pp. 70–76, 2024.

[12] D. P. K. Tabanan, "Penelitian Penerapan Parkir Elektronik dan Tarif Parkir Tahun 2017," Tabanan, 2017.

[13] I. G. F. . Tapa, I. N. . Kumara, and D. . Indrashwara, "Evaluasi Kelayakan Finansial Penerapan Terminal Parkir Elektronik Pada On Street Parking Di Kota Tabanan (Studi Kasus: Jalan MH Thamrin Kediri-Tabanan)," *J. Ilm. Poli Rekayasa*, vol. 18, no. 2, pp. 59–67, 2023.

[14] S. Husnan, *Studi Kelayakan Proyek*, Edisi Keem. Yogyakarta: UPP STIM YKPN, 2000.

[15] Asiyanto, *Manajemen Biaya Proyek Konstruksi*. Jakarta: Pradnya Paramita, 2005.

[16] M. Adler and B. Dumas, "Paparan Risiko Mata Uang: Definisi dan Pengukuran," *Manaj. Keuangan/Musim Panas*, 1982.

Matrix: Jurnal Manajemen Teknologi dan Informatika
Volume 15 Issue 1 Year 2025 Pages 9-20
DOI: http://dx.doi.org/10.31940/matrix.v15i1.9-20
URL: http://ojs2.pnb.ac.id/index.php/matrix

Data acquisition of flow sensor based to measure water flow in underground drainage

I Made Adiswara Wirama [1]*, Rusminto Tjatur Widodo [2], Muhammad Udin Harun Al Rasyid [3], Hary Oktavianto [4]

[1,2,4] *Faculty of Electrical Engineering, Politeknik Elektronika Negeri Surabaya, Indonesia*
[3] *Faculty of Informatics and Computer Engineering, Politeknik Elektronika Negeri Surabaya, Indonesia*

*Corresponding Author: *ramawiramas@gmail.com*

Abstract: This research focuses on water flow sensors in underground drainage. In Indonesia, the use of sensors and actuators to control and measure water velocity and water discharge in underground drainage is not very popular, although one of the causes of flooding is caused by clogged drainage or workers forgetting to turn on the pump at a certain height and water flow. This paper will explain how to find out the speed and discharge of water in an underground drainage without checking it directly on site. The water flow sensor is used to measure the water velocity and water discharge entering a drainage system. The data acquisition conducted with 3 section, data preparation, data collecting, and data processing. Data preparation is preparing the microcontroller, sensor, and data display to get the data. Data collecting is about collecting the data from sensor in this research the data collected is in pulse that can be calculated to water discharge and water velocity in the data processing. From the experiment, it can be seen that the highest error rate on the sensor is 7.64% and the lowest at 0% or no error with the average amount of error is 2.46%. The data obtained from the sensor can be converted into water velocity and water discharge depending on the shape of the drainage. The length, width and height of the drainage are assumed to be 10x4x3 m respectively, with a constant water level of 2 m, so the water flow sensor is placed at a height of 1 m because the safe height is 1 m. From the case study conducted the error rate of the water flow sensor error is 0%, because the case study conducted using imaginary data. Based from this, the knowledge gained from the research, it can be used to determine the water velocity and water discharge value of underground drainage using water flow sensor, which is expected to be applied to pump houses to more easily determine the state of drainage.

Keywords: microcontroller, sensor, underground drainage, water discharge, water velocity

History Article: Submitted 16 February 2025 | Revised 17 March 2025 | Accepted 22 April 2025

How to Cite: I. M. A. Wirama, R. T. Widodo, M. U. H. Al Rasyid, and H. Oktavianto, "Data acquisition of flow sensor based to measure water flow in underground drainage", *Matrix : Jurnal Manajemen Teknologi dan Informatika*, vol. 15, no. 1, pp. 9–20, 2025. doi.org/10.31940/matrix.v15i1.9-20.

Introduction

Flood is one of the disasters that can be caused by human negligence towards their environment, especially flood that occurs on the highway. Because the occurrence of flood in the road, it can hinder the flow of traffic in which will cause traffic jams. Therefore, it is necessary to reduce or mitigate flood on the highway, where one way is to make drainage. At 2023 flood is the third most occurring disaster in Indonesia [1].

Drainage is defined as a means of draining or disposing of water that is used to reduce excess water in an area so that the area is not flooded. The excess water can come from rainwater, seepage, or excess irrigation water. Drainage can be surface or subsurface. Underground drainage is a man-made structure built underground under roads or beside rivers. In addition, underground drainage also has the function of draining the water above it and directing it to the river [2].

One of the parameters that can be measured in the underground drainage is the water flow in the underground drainage. Knowing the speed of water flow is very important, by knowing the speed of water flow in the underground drainage, it can estimate the blockage in the drainage and estimate the water discharge parameter, so it can open the pump to direct

water from the drainage to another drainage or the nearest river. In this way, it can mitigate the flood before it even happens.

Previously there have been other researches to check the state or condition of underground drainage such as monitoring underground drainage using ultrasonic sensor to determine the water level of the drainage [3], [4], [5], [6], [7], [8]. Using the gas sensor to check the condition of the underground drainage [9]. Many researcher is using the flow sensor to find the water velocity and water discharge [10], [11], [12], [13], [14]. None of these researches explain the water flow rate, nor the water discharge rate by utilizing the dimensions of the underground drainage. So the research in this paper is to measure the parameters of water flow rate and water discharge using a water flow sensor. This water flow sensor uses hall-effect technology to estimate the water flow rate. From the water flow rate obtained and the estimated drainage dimensions, the amount of water flowing in the drainage can be determined.

Methodology

Data acquisition on the water flow sensor is carried out to determine the speed of water flow and water discharge in the underground drainage. data obtained from the flow of water in the underground drainage and then processed through the water flow sensor using the Arduino UNO microcontroller and then the processed data is displayed using an OLED screen. Figure 1 illustrates the block diagram of the data acquisition process from the underground drainage to the OLED screen or its output.

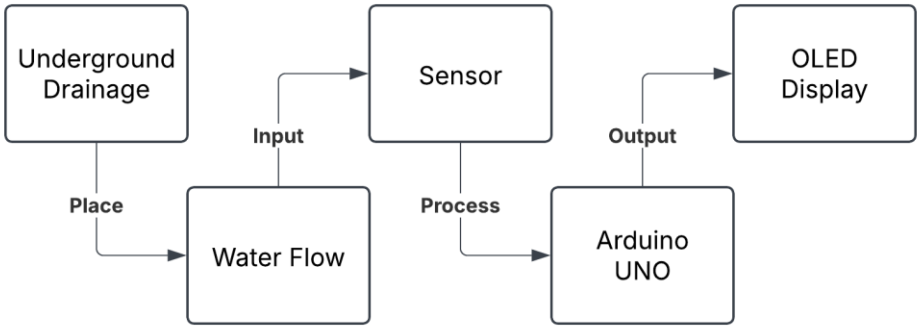

Figure 1. Block diagram

In Figure 1, the block diagram of the system is started from the place or location, then the flow sensor gets the data from the water in the underground drainage. The data obtained from the sensor then processed with microcontroller. After that the output of data that processed in microcontroller is displayed in OLED display.

From the block diagram the microcontroller used is Arduino UNO, it can be seen in Figure 2 (a). For the flow sensor it used YF-S201 water flow sensor to obtained the water data, the image of this sensor is in Figure 2 (b). Lastly, for the display it used OLED 128X64 display, this is in Figure 2 (c). The schematic of this project can be seen in Figure 3. From the microcontroller pinouts, this module requires a voltage of 5V to operate. This module also uses 1 digital pinout, and 2 ADC pinouts.

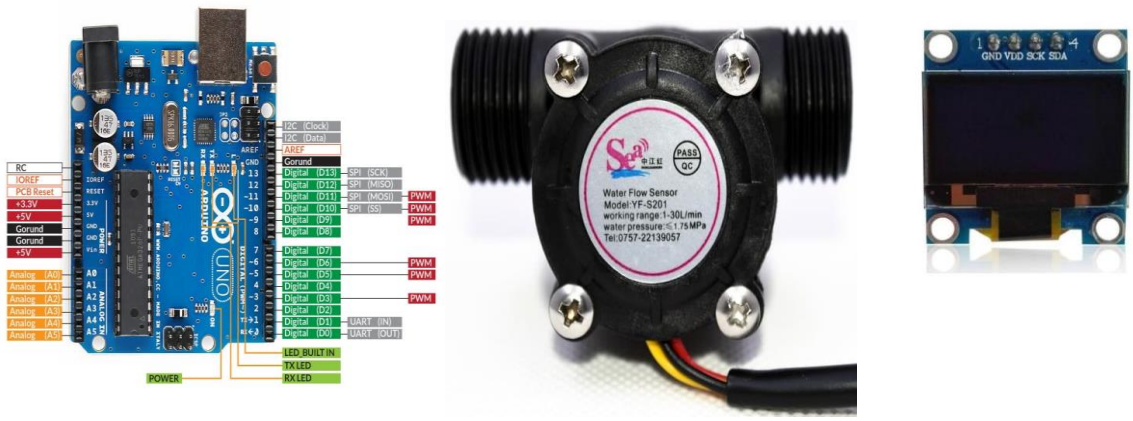

(a) (b) (c)

Figure 2. (a) Arduino UNO, (b) YF-S201, (c) 128X64 OLED Display

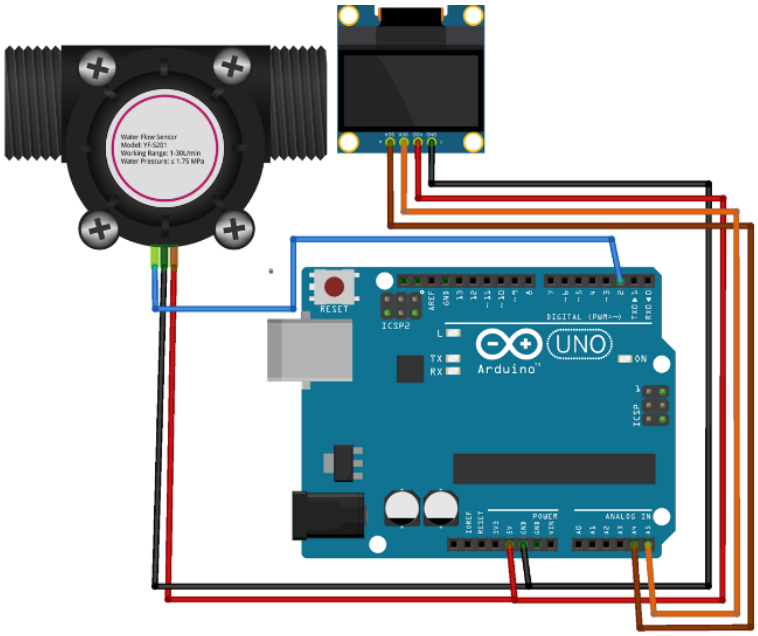

PIN LABEL	
YF-S201	**UNO**
GND	GND
VCC	5V
SIG	D2

PIN LABEL	
128X64 OLED	**UNO**
GND	GND
VDD	5V
SCK	A5
SDA	A4

Figure 3. Wiring diagram of water flow data acquisition

To understand how the water flow sensor work and how the data being acquisition it can be seen in Figure 4.

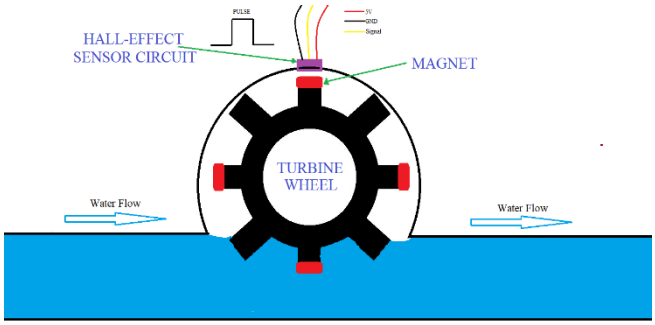

Figure 4. YF-S201 working principle

The water flows into the pipe on the sensor, which is then detected by hall effect technology on the sensor using turbine wheel. From Figure 4, there are 4 magnets in turbine wheel indicated by the color red. Every time the hall-effect detect the magnet it will increase the pulse by one, or

equal to 1 pulse. That mean the speed of turbine wheel depends on the speed of the water flowing through the pipe [15].

After that is data acquisition, data acquisition is divided into 3 sections it is data preparation, data collecting, and data processing. The first step is data preparation, data Preparation section prepares the tools that will be used to perform the experiments. For data acquisition, the tools prepared in the previous section are described here, namely microcontrollers, sensors, and data display screens as it can be seen in Figure 3. For the place where the test will be carried out for now, it will still be carried out using a faucet to measure the speed of the water flow and the incoming water discharge depending on the number of impulses obtained in a certain period of time.

The next section is data collecting, this section is about collecting the data is with tools that already prepared in the previous section. In this research data collection is done using a water flow sensor on the microcontroller. The data is collected by connecting the sensor with a water tap using a hose in simulated condition. Conditions are simulated by turning the used water tap at different speeds within a given time. In this way, different impulse values and volumes of water are obtained in the same period of time. The measurement error rate of this sensor based from the data sheet is estimate to be around 10 or 5% and it is already enough precision for this research. The parameter obtained from this test is pulse, water volume, and frequency.

In order to determine whether the sensor used is working properly, a measurement test of the sensor is performed by experimenting twice on the same volume of water at the same height of the measuring cup in 15 seconds. To find the error value of each experiment and the average error of all experiments, Equation (1) and Equation (2) are used.

$$error = \left| 100 - \left(\left(\frac{f1}{f2} \right) 100 \right) \right| \quad (1)$$

$$\overline{error} = \frac{\sum error}{N_{Test}} \quad (2)$$

Where $f1$ is first test frequency (Hz), $f2$ is second test frequency (Hz), N_{Test} is the number of test conducted, $error$ is number of error (%) and $\overline{error}$ is average of total error (%)

Data processing is the third section of data acquisition, where the previously collected data is converted into parameters that will be used in the case study to prove the formulas used is correct. For this research, the frequency parameters obtained in the previous stage are converted into water discharge and water flow parameters.

After data acquisition, the parameters obtained are tested on a case study with random parameters with the limitations of the sensors used. for this experiment, the length, width and height of the drainage are 10x4x3 m. The length of the drainage is more than 100 m, but only the area within the 10 m will be calculated. The height of the water in drainage is assumed to be constant at 2 m, so the sensor is placed at a height of 1 m from the bottom of the drain. In the case study the limit of water flow velocity is 720 L/H or 12 L/minute using the linear exponential graph of the water flow sensor obtained from the sensor datasheet show in Figure 5.

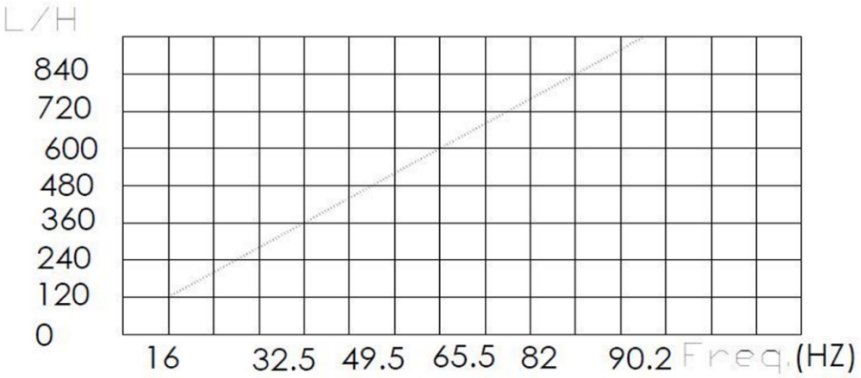

Figure 5. Flow Sensor Exponential Linear Graph

By looking at the graph in Figure 5, a table can be made that determines the relationship between frequency and water discharge. The relationship can be seen in Table 1.

Table 1. Frequency comparison with water discharge

Discharge(L/H)	Frequency(Hz)
120	16
240	32.5
360	49.3
480	65.5
600	82
720	90.2

Table 1 shows the comparison obtained from the linear exponential graph in Figure 5. This comparison is a benchmark for finding the water discharge with the frequency data obtained previously. The formula for finding the water discharge can be obtained by linear interpolation of two comparison data that are close to the frequency obtained. The formula is shown in Equation (3).

$$Q_x = Q_1 + \frac{(f_x - f_1)(Q_2 - Q_1)}{(f_2 - f_1)} \tag{3}$$

Where Q_x is interpolated water discharge (L/H), f_x is interpolated frequency (Hz), Q_1 is f_1 water discharge (L/H), f_1 is frequency smaller than f_x (Hz), Q_2 is f_2 water discharge (L/H) and f_2 is frequency bigger than f_x (Hz).

By knowing the formula for finding the water discharge, the speed of water flow can be found. To find the water flow velocity, the cross-sectional area through which the water flows and the water discharge are required. With the previous explanation, the water flow velocity can be found by using the continuity equation. Before executing the continuity equation, the hour unit on the water discharge from the results of Equation (3) must be converted to seconds by dividing by 3600. With the previous explanation, it can be seen in the formula Equation (4).

$$v = \frac{Q/_{3600}}{A} \tag{4}$$

Where v is water velocity (m/s), Q is water discharge (L/H), meanwhile A is water cross-section area (m^2).

The design of this project utilize Arduino IDE as it software tool. Arduino IDE is used to programmed Arduino IDE in the project. The program consists of receiving input from the flow sensor and displaying the pulse received in the flow sensor in the OLED display. Figure 6 display the code, library and syntax used in programming this project.

```
//Libraries
#include <Adafruit_GFX.h>
#include <Adafruit_SSD1306.h>
// OLED I/O
#define SCREEN_WIDTH 128 // OLED display width, in pixels
#define SCREEN_HEIGHT 64 // OLED display height, in pixels
#define OLED_RESET -1 // Reset pin # (or -1 if sharing Arduino
reset pin)
Adafruit_SSD1306 display(SCREEN_WIDTH, SCREEN_HEIGHT, &Wire,
OLED_RESET);
//Define Sensor Pin
#define flowPin 2
volatile int count;
void setup() {
  //read pin
  if(!display.begin(SSD1306_SWITCHCAPVCC, 0x3C)) { // Address 0x3C
for 128x32
    Serial.println(F("SSD1306 allocation failed"));
    for(;;); // Don't proceed, loop forever
  }
  pinMode(flowPin, INPUT);

  //Another Configuration
  attachInterrupt(digitalPinToInterrupt(flowPin), Flow, RISING);
  Serial.begin(115200);
}
```

```
void loop() {
  interrupts();   //Enables interrupts on the Arduino
  display.clearDisplay();
  display.setTextSize(4);             // Normal 1:1 pixel
scale
  display.setTextColor(WHITE);        // Draw white text
  display.setCursor(0,0);             // Start at top-left
corner
  display.print("Pulse:");
  display.println(count);
  display.display();
  Serial.println(count);
}

//Interrupt Count Sensor
void Flow(){
  count++;
}
```

Figure 6. The code of this project in Arduino IDE

Results and Discussions

Data acquisition in this project conducted in 3 step data preparation, data collection, and data processing. In every step the experiment is conducted to ensure the data obtained is not full of error.

Sensor Calibration

To ensure the flow sensor work correctly, an experiment is needed to prove that the equation before is correct by displaying the frequency pulse signal using an oscilloscope. In this experiment, the oscilloscope settings used are 5V for Volt/Div, 10ms Time/Div. The voltage is set to 5V because the highest voltage is at 5V, so it is easy to calculate div. The time is set to 10ms because the signal is clearly visible on the oscilloscope. The signal can be seen in Figure 7, the signal obtained is in the form of a step signal.

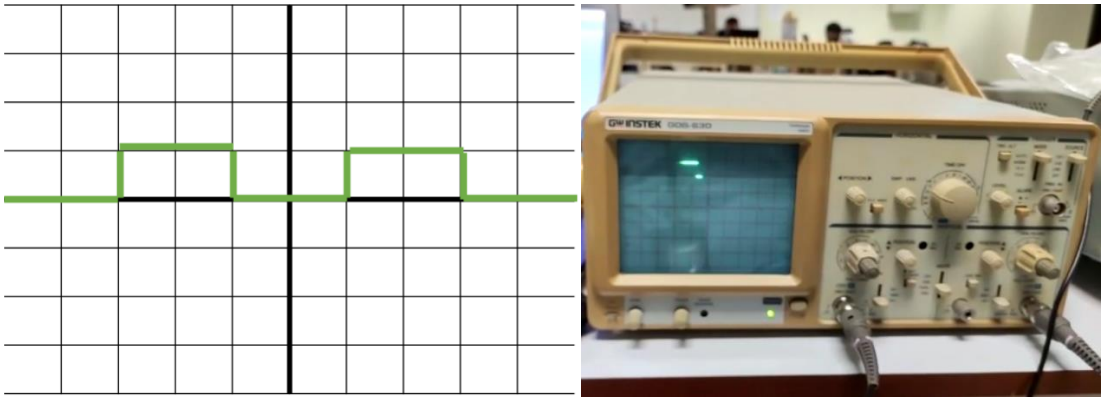

Figure 7. Oscilloscope signal

From the signal, it can be seen that one period is 4 Div, so to find the signal time, Time/Div set previously is multiplied by number of Div for one period (T) to get a time of 40ms. Because the time has been obtained, the frequency can be found using the Equation (5).

$$f = \frac{1}{T} \tag{5}$$

From the Equation (5) the frequency obtained is 25 Hz. Because Div in Volt/Div is only 1 Div, the voltage obtained is 5V. The frequency obtained will continue to decrease over time as the water tap is turned down until it closed as seen at the graph in Figure 8. It can be seen that the water flow velocity will continue to decrease as the water tap turned down more and more until it fully closed.

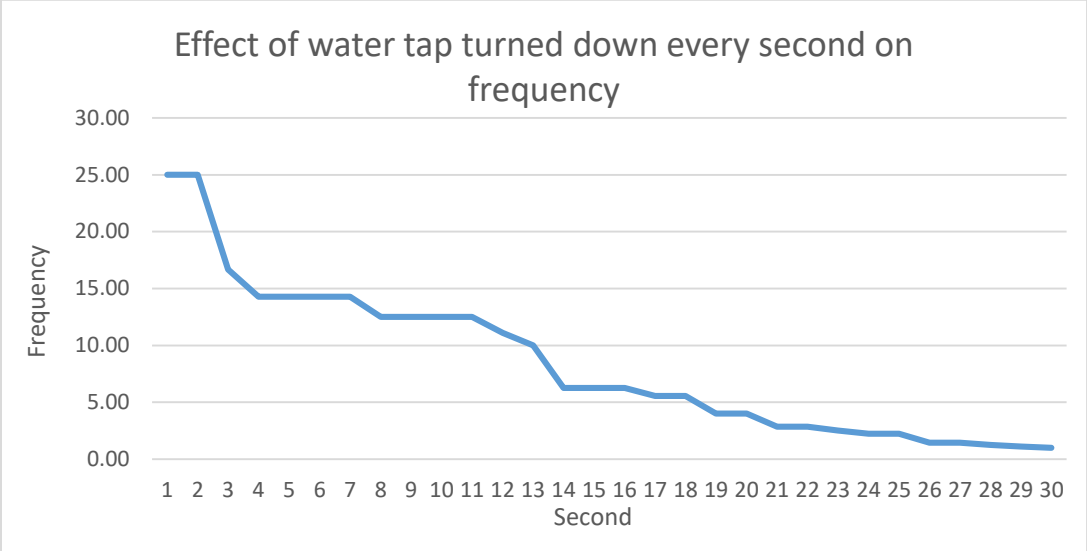

Figure 8. Effect of water tap closed slowly every second.

The parameter values of the graph can be seen in Table 2, which shows the effect of time (ms) on the frequency obtained. It can also be seen that the frequency value decreases the longer the faucet of the calibration tool is open. This is because the more water that comes out of the faucet, the more the volume of water in the calibration tool decreases, causing a decrease in the frequency detected.

Table 2. Frequency obtained over time

No (s)	Time/ Div	Div	Time (ms)	Frequency (Hz)
1	10	4	40	25.00
2	10	4	40	25.00
3	10	6	60	16.67
4	10	7	70	14.29
5	10	7	70	14.29
6	10	7	70	14.29
7	10	7	70	14.29
8	10	8	80	12.50
9	10	8	80	12.50
10	10	8	80	12.50
11	10	8	80	12.50
12	10	9	90	11.11
13	10	10	100	10.00
14	20	8	160	6.25
15	20	8	160	6.25

Data Collection

Based from the explanation in the methodology about data collection, the data collecting conducted can be seen in Figure 9 to get the pulse data.

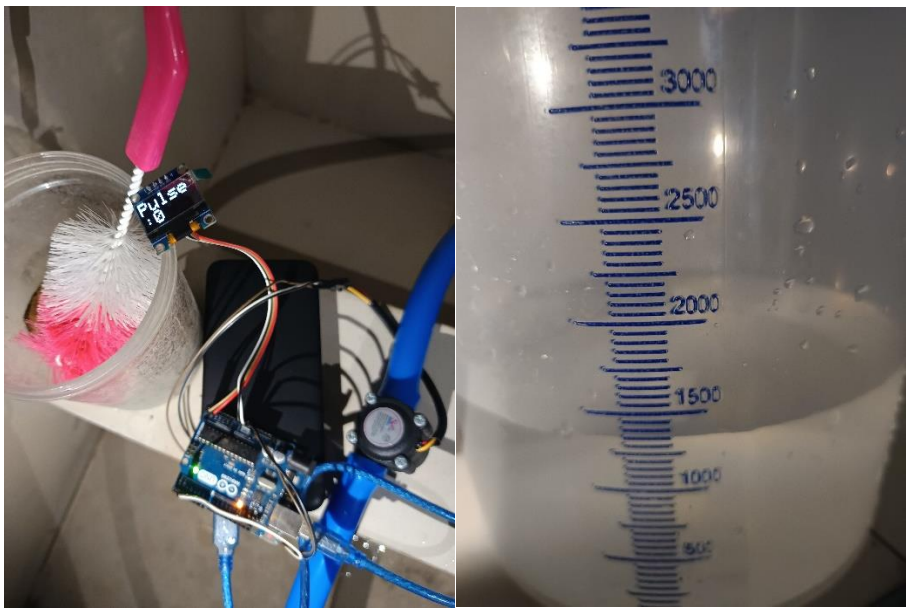

Figure 9. Data collection with water flow sensor

In Figure 9, the experiment was conducted on the direct sensor. The data collected in the experiment are two: pulse data and water volume data. The pulse data is obtained from the direct sensor, and the water volume data is obtained from the measuring cup. The first experiment was carried out by looking for pulses with a specified volume of water within 15 seconds. This experiment was repeated 25 times with different volumes to determine the number of errors and the average error of the sensor used. The second experiments were conducted in different time periods, namely 5 seconds, 7 seconds, 10 seconds and 12 seconds. By obtaining the parameters of the pulse and water volume, it can be find the frequency parameter using the formula on Equation (6). The obtained parameters are shown in Table 3 and Table 4.

$$f = \frac{x}{t} \tag{6}$$

Where f is frequency (Hz), x is pulse and t represent time (s).

Table 3. Experimental data from the calibration test in 15 seconds

No	Water Volume (mL)	Pulse 1	Pulse 2	Frequency 1 (Hz)	Frequency 2 (Hz)	Error (%)
1	600	325	343	21.67	22.87	5.25
2	650	373	378	24.87	25.20	1.32
3	700	405	398	27.00	26.53	1.76
4	750	425	410	28.33	27.33	3.66
5	800	455	461	30.33	30.73	1.30
6	850	509	488	33.93	32.53	4.30
7	900	522	522	34.80	34.80	0.00
8	950	579	551	38.60	36.73	5.08
9	1000	605	611	40.33	40.73	0.98
10	1050	613	631	40.87	42.07	2.85
11	1100	645	667	43.00	44.47	3.30

No	Water Volume (mL)	Pulse 1	Pulse 2	Frequency 1 (Hz)	Frequency 2 (Hz)	Error (%)
12	1150	679	644	45.27	42.93	5.43
13	1200	688	701	45.87	46.73	1.85
14	1250	713	722	47.53	48.13	1.25
15	1300	735	736	49.00	49.07	0.14
16	1350	785	787	52.33	52.46	0.23
17	1400	815	801	54.33	53.40	1.75
18	1450	811	845	54.07	56.33	4.02
19	1500	873	811	58.20	54.07	7.64
20	1550	902	904	60.13	60.27	0.22
21	1600	932	921	62.13	61.40	1.19
22	1650	961	991	64.07	66.07	3.03
23	1700	965	993	64.33	66.20	2.82
24	1750	1004	1022	66.93	68.13	1.76
25	1750	1049	1052	69.93	70.13	0.29
Error Average						2.46

Using Equation (1) and Equation (2), we can find the error and average error from the data obtained in Table 3. In the table, the highest amount of error is 7.64% at 1500 ml water volume and the lowest amount of error is 0% or no error at 900 ml water volume. By averaging the number of errors from the total error obtained in 25 experiments, the amount found is 2.46%. According to the data sheet, if the error does not exceed 10%, the sensor can still be properly used.

Table 4. Experimental data at various time intervals

Time (s)	Pulse	Water Volume (mL)	Frequency (Hz)
5	387	750	77.40
5	325	600	65.00
5	405	1050	81.00
5	386	600	77.20
5	425	650	85.00
5	397	700	79.40
7	411	800	58.71
7	309	600	44.14
7	427	800	61.00
7	338	650	48.29
7	368	750	52.57
7	407	750	58.14
10	713	1350	71.30
10	262	450	26.20
10	579	1150	57.90
10	613	1150	61.30
10	455	900	45.50
10	523	1000	52.30

Time (s)	Pulse	Water Volume (mL)	Frequency (Hz)
12	673	1300	56.08
12	679	1300	56.58
12	1047	2050	87.25
12	878	1800	73.17
12	605	1100	50.42
12	725	1500	60.42

Data Processing

With the data obtained in Table 4, data processing is then performed on the frequency obtained in the previous data, which can be seen in Table 5.

Table 5. Processed data of water discharge by time interval

Time (s)	Frequency (Hz)	Water Discharge (L/h)
5	58.71	429.7354497
5	44.14	323.1632653
5	61.00	446.6666667
5	48.29	352.755102
5	52.57	384.2328042
5	58.14	425.5026455
7	58.71	429.7354497
7	44.14	323.1632653
7	61.00	446.6666667
7	48.29	352.755102
7	52.57	384.2328042
7	58.14	425.5026455
10	71.30	522.1818182
10	26.20	194.1818182
10	57.90	423.7037037
10	61.30	448.8888889
10	45.50	332.8571429
10	52.30	382.2222222
12	56.08	410.2469136
12	56.58	413.9506173
12	87.25	676.8292683
12	73.17	535.7575758
12	50.42	368.2716049
12	60.42	442.345679

From Table 5 it can be seen that there is no water flow, this is because the area is not known, so Equation (4) cannot be used to obtain the parameters. For more depth, a case study is carried out with the shape of the sensor area.

Case Study

The shape of the underground drainage in this case study is shown in Figure 10. From the real image of the drainage system, it was converted into a schematic diagram to facilitate calculation. From the explanation of the methodology, it can be seen that the underground drainage is in the form of a beam, so the area of this drainage can be obtained using Equation (7) and the water volume can be obtained by multiplying the long, wide, and height.

$$L = 2[(l \times w) + (l \times h) + (h \times w)] \quad (7)$$

Where L is water cross-sectional area (m^2), l is water long (m), w is water wide (m) and h is water height (m)

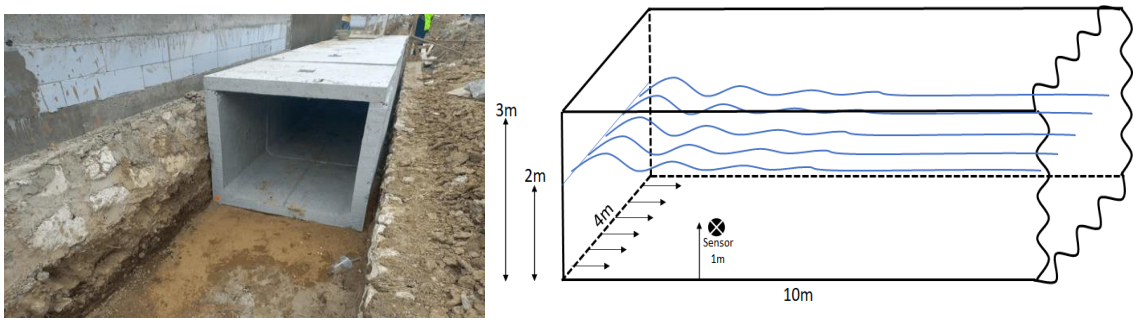

Figure 10. Underground drainage shape

After obtaining the area and the water volume, the experiment can be carried out by trying to enter the randomized pulse parameter 10 times for comparison. With the known parameters of area, water volume and pulse, we can find the water discharge with Equation (3) and water flow with Equation (4), the results can be seen in Table 6.

Table 6. Case study result

No	Pulse	Wtr Vol (Ltr)	Wtr Area (m^2)	Freq (Hz)	Wtr Discharge (L/H)	Wtr Flow (m/s)
1	1964	80	136	32.73	241.6666667	0.000493600
2	3753	80	136	62.55	458.1481481	0.000935760
3	5024	80	136	83.73	625.3658537	0.001277300
4	1663	80	136	27.72	205.2121212	0.000419142
5	2701	80	136	45.02	329.4047619	0.000672804
6	4876	80	136	81.27	589.2682927	0.001203571
7	3877	80	136	64.62	473.4567901	0.000967028
8	2257	80	136	37.62	276.5476190	0.000564844
9	2812	80	136	46.87	342.6190476	0.000699794
10	4528	80	136	75.47	504.3902439	0.001030209

From Table 6 it can be seen that the result of the previous calculation based from 10 imaginary number randomly selected for the pulse. Because it still in imaginary number the test is still 0% error if it based from the equation.

Conclusion

Data acquisition for underground drainage was performed. From the calibration of the water flow sensor, it can be proved that the frequency obtained when the water tap closes becomes smaller, which is proved by experiments with an oscilloscope. From the above experiment, it can be seen that the highest error rate on the sensor according to Table 3 is 7.64% and the lowest at 0% or no error with the average amount of error is 2.46%. Through this experiment, the sensor can be used to find the water discharge by using the frequency obtained from Equation (6). From the results, the water discharge can be found by linear interpolation by comparing two coordinates that are close to the frequency obtained according to Table 5. Then, the water flow velocity can be found with the obtained water discharge. For this case study, there is no average error because the use of formulas in calculations does not use sensors, but uses random data. In future research, water level sensors can be added and direct experiments on underground drainage can be conducted to obtain more complete research results.

References

[1] Badan Pusat Statistik, "Jumlah Bencana Alam Menurut Provinsi dan Jenis Bencana Alam (kejadian), 2024". [Online]. Available: https://www.bps.go.id/id/statistics-table/3/TUZaMGVteFVjSEJ4T1RCM%20lIyRjRTazVvVDJocVFUMDkjMw==/jumlah-kejadian-bencana-alam-menurut-provinsi.html?%20year=2023

[2] E. Tri *et al.*, "Drainase Perkotaan," 2021. [Online]. Available: www.rcipress.rcipublisher.org

[3] Mc. Kumar Naidu, Nn. Chowdary, Ln. Sai, and Pv. Krishna, "Smart Drainage Monitoring System Using IoT".

[4] Bhuvaneshwaran A, "Iot Based Drainage and Waste Management Monitoring and Alert System for Smart City," *Ann Rom Soc Cell Biol*, vol. 25, no. 3, pp. 6641–6651, 2021, [Online]. Available: http://annalsofrscb.ro

[5] G. Sonawane, C. Mahajan, A. Nikale, and Y. Dalvi, "Smart Real-Time Drainage Monitoring System Using Internet of Things," 2018.

[6] T. Pathak, S. Deshmukh, P. Reddy, and H. P. Rewatkar, "Smart Drainage Monitoring and Controlling System Using IOT." [Online]. Available: www.ijres.org

[7] S. Abdulhayan, R. Sharma, P. Ainapur, S. Sanjay Wadakar, and A. Professor, "Underground Drainage Monitoring System," *IJSDR1905040 International Journal of Scientific Development and Research*, 2019, [Online]. Available: www.ijsdr.org

[8] D. Deepak Kumar and V. Jayaprakasan, "Urban underground drainage monitoring system using IoT," 2021. [Online]. Available: https://www.ijariit.com

[9] C. G, C. B, K. P, B. sasi, and Prof. V. K. Kumar, "IoT Based Underground Drainage Monitoring System," *International Journal of Recent Technology and Engineering (IJRTE)*, vol. 9, no. 3, pp. 247–249, Sep. 2020, doi: 10.35940/ijrte.C4354.099320.

[10] K. Viswanadh, P. Rojitha, S. K. Khadija, S. M. S. P. C. Venkataraju, P. Nagamani, and U. G. Student, "Under Ground Drainage Monitoring System Using IoT," 2019. [Online]. Available: www.jetir.org

[11] M. Gunasekaran, Pavithra S, Priyanka R, and Reeva M, "IoT-Enabled Underground Drainage Monitoring System Using Water Flow Sensor," *International Research Journal of Engineering and Technology*, p. 2427, 2008, [Online]. Available: www.irjet.net

[12] T. S. Arulananth, G. Ramya Laxmi, K. Renuka, and K. Karthik, "Smart sensors and arm based drainage monitoring system," *International Journal of Innovative Technology and Exploring Engineering*, vol. 8, no. 11 Special Issue, pp. 997–999, Sep. 2019, doi: 10.35940/ijitee.K1183.09811S19.

[13] R. Hartono, S. Alim Tri Bawono, M. Asri Safi, A. Aziz, F. Aji Purnomo, and M. Alfiandoko, "Optimasi Penggunaan Sensor Water Flow HF-S201 Guna Mengukur Aliran Air Mendukung Mitigasi Banjir," 2021.

[14] "Rancang Bangun Alat Pengukur Kecepatan Aliran Air Menggunakan Water Flow Sensor Berbasis Ardunino Uno Formateks".

[15] A. Suharjono, L. N. Rahayu, and R. Afwah, "Aplikasi Sensor Flow Water Untuk Mengukur Penggunaan Air Pelanggan Secara Digital Serta Pengiriman Data Secara Otomatis Pada PDAM Kota Semarang," 2015.

Matrix: Jurnal Manajemen Teknologi dan Informatika
Volume 15 Issue 1 Year 2025 Pages 21-31
DOI: http://dx.doi.org/10.31940/matrix.v15i1.21-31
URL: http://ojs2.pnb.ac.id/index.php/matrix

Analysis of corn production in Indonesia using business intelligence technology based on Power BI

Muh Kevin Adesyahputra [1]*, Eka Putri Rachmawati [2]

[1,2] *Information Systems, Universitas Semarang, Indonesia*

*Corresponding Author: *muhkevinadesyahputra@gmail.com*

Abstract: Corn production trends in Indonesia from 2020 to 2024 were analyzed to address regional disparities and enhance data-driven agricultural decision-making. Datasets from the Ministry of Agriculture and the Central Bureau of Statistics were integrated, transformed, and visualized using Microsoft Power BI, with a focus on evaluating fluctuations in harvested area, production volume, and productivity. Key objectives included identifying challenges linked to fragmented data and external disruptions. An Extract-Transform-Load (ETL) framework harmonized pre-2023 and post-2023 datasets, enabling standardized comparisons across 38 provinces. Results indicated a production peak of 486,000 tons in 2022, followed by a 4.5% decline in 2023 due to adverse climatic conditions and supply chain instability, and partial recovery to 15.2 million tons in 2024. Pronounced regional disparities emerged: West Java recorded 80 quintals per hectare productivity, while urbanized regions like Jakarta reported negligible output. The analysis underscores the efficacy of Business Intelligence (BI) tools in converting raw agricultural data into strategic insights, offering policymakers pathways to optimize resource allocation, mitigate inequities, and strengthen climate-resilient practices. These outcomes highlight BI's transformative potential in advancing sustainable agricultural development and adaptive governance frameworks.

Keywords: business intelligence, corn production, data analytics, ETL, Power BI

History Article: Submitted 6 January 2025 | Revised 26 March 2025 | Accepted 15 April 2025

How to Cite: M. K. Adesyahputra and E. P. Rachmawati, "Analysis of corn production in Indonesia using business intelligence technology based on Power BI", *Matrix : Jurnal Manajemen Teknologi dan Informatika*, vol. 15, no. 1, pp. 21–31, 2025. doi.org/10.31940/matrix.v15i1.21-31.

Introduction

Indonesia, as one of Southeast Asia's largest agricultural producers, plays a critical role in regional food security and economic stability [1]. Agriculture significantly contributes to the nation's GDP, employment, and socio-economic development. Among its key agricultural commodities, corn holds strategic importance as a dual-purpose crop: it serves as a staple food source for millions and a primary ingredient in livestock feed production [2]. Efficient corn production management is essential to ensure food security, support the livestock sector, and drive sustainable economic growth [3].

Despite its significance, Indonesia faces persistent challenges in optimizing corn production. Agricultural data crucial for policymaking are often fragmented, multidimensional, and inconsistently formatted across regions [4]. This lack of standardization hinders stakeholders from leveraging data effectively, resulting in suboptimal resource allocation, uneven productivity, and stark regional disparities [5]. External factors such as climate change, supply chain disruptions, and market volatility further complicate production planning, adding layers of complexity to agricultural management [6].

Technological advancements in information systems, particularly Business Intelligence (BI), offer transformative solutions. BI tools like Microsoft Power BI enable the integration, transformation, and visualization of complex datasets, empowering stakeholders to make data-driven decisions [7]. For instance, Microsoft Power BI a BI platform facilitates the creation of interactive dashboards and real-time analytics, allowing users to explore data dynamically [8]. Modern BI tools incorporate OLAP (Online Analytical Processing), a data analysis technique that organizes information rapid querying and aggregation, enabling stakeholders to dissect

agricultural datasets across critical dimensions such as region, time period, and production scale and systematically uncover latent patterns and trends essential for strategic decision-making [9]. Together, these IT innovations empower users to identify trends, detect inefficiencies, and make data-driven decisions across a wide range of sectors, including agriculture [6].

Corn production in Indonesia is influenced by multiple interrelated factors, including harvested area, productivity per hectare, access to farming technologies, and external conditions such as weather and market dynamics [10]. Each of these factors contributes to the overall production landscape, and understanding their interactions requires sophisticated data analysis methods [4]. For instance, disparities in productivity between provinces are often linked to unequal access to resources such as high-quality seeds, fertilizers, and irrigation systems. Similarly, technological adoption, government support, and infrastructure availability play a crucial role in determining the efficiency of agricultural activities in different regions. Addressing these disparities is essential to achieving equitable development and ensuring that all regions can reach their full potential.

To tackle these challenges, this study focuses on applying Business Intelligence to analyze corn production data in Indonesia during the 2020–2024 period. The integration of Business Intelligence with large-scale agricultural datasets has been shown to enhance decision-making capabilities by leveraging advanced data processing and real-time analytics [11]. Microsoft Power BI is employed to process, analyze, and visualize the data, providing stakeholders with an intuitive and interactive platform to explore production trends and regional disparities. The research methodology incorporates an Extract, Transform, Load (ETL) process to ensure the accuracy, consistency, and reliability of the data. This process involves extracting data from official statistical sources, transforming it into a standardized format, and loading it into a BI platform for comprehensive analysis [12]. The OLAP-like features integrated within Power BI enhance the analysis by enabling users to drill down into detailed data dimensions, compare metrics across regions and time periods, and aggregate results at varying levels of granularity [9]. Using Power BI dashboards, stakeholders can interactively explore key metrics such as harvested area, production volume, and productivity per hectare across different regions [7]. These visualizations highlight patterns, identify underperforming regions, and enable targeted interventions to address productivity gaps.

Beyond addressing agricultural challenges, this study emphasizes the broader role of advanced information systems in revolutionizing data management across various domains. Traditional methods of data analysis often rely on static reports and manual processing, which are time-consuming and prone to errors. In contrast, BI tools offer dynamic and automated solutions that significantly enhance the accessibility and usability of data [6]. By transforming raw data into actionable visual insights, these platforms enable stakeholders to make informed decisions based on real-time information. This capability is particularly valuable in a rapidly changing environment where timely and accurate data is essential for effective decision-making [13].

The integration of Business Intelligence into agricultural data management not only improves operational efficiency but also fosters collaboration among various stakeholders. Government agencies, private organizations, and local communities can leverage shared digital platforms to coordinate efforts, align strategic goals, and implement policies that address systemic challenges [14]. For example, insights derived from Power BI dashboards can guide policymakers in designing programs to support underperforming regions, allocate resources more effectively, and mitigate the impacts of external disruptions such as climate change and market volatility. This collaborative approach ensures that decision-making is inclusive, data-driven, and aligned with the broader goals of sustainable development.

Furthermore, this research highlights the potential of advanced information systems to drive innovation and sustainability in agriculture. By providing clear, data-driven insights, BI tools enable stakeholders to identify inefficiencies, optimize resource allocation, and develop strategies that promote resilience and adaptability [15]. This aligns with global efforts to achieve sustainable development goals, particularly those related to food security, economic growth, and environmental sustainability. The application of BI in agricultural data management demonstrates how cutting-edge technology can be harnessed to address complex challenges, unlock new opportunities, and improve the overall efficiency of critical sectors [6].

Ultimately, this study underscores the transformative power of information systems in enabling data-driven decision-making. By leveraging Microsoft Power BI to analyze and visualize corn production data, the research provides a blueprint for integrating advanced IT solutions into agricultural management practices [15]. The findings aim to equip stakeholders with actionable insights that can guide evidence-based strategies to enhance productivity, address regional disparities, and strengthen the resilience of Indonesia's agricultural sector. Moreover, the study serves as a testament to the broader relevance of modern information systems in driving innovation, fostering collaboration, and supporting sustainable development across diverse sectors.

Methodology

This study analyzes corn production data in Indonesia for the period 2020–2024 using a Business Intelligence approach based on Microsoft Power BI. Data were collected from official reports issued by the Ministry of Agriculture and the Central Bureau of Statistics (BPS). The process begins with the collection of secondary data on corn production, harvested area, and productivity from these official sources.

After collection, the next stage is the Extract, Transform, Load (ETL) process. In the extraction phase, data from two different periods (2020–2022, referred to as the Pre-2023 Dataset, and 2023–2024, referred to as the Post-2023 Dataset) are obtained. In the transformation phase, the two datasets are merged into one unified dataset. Common fields (for example, year, province, harvested area, production volume, and productivity) are aligned so that both datasets share the same column structure. Duplicate rows are removed to maintain data accuracy, and missing values for provinces not established in 2020–2022 are set as NULL or zero. Data gaps for newly established provinces in 2023–2024 are clearly marked, and province names are standardized across both periods to ensure consistency. In the loading phase, the cleansed and merged dataset is imported into Microsoft Power BI.

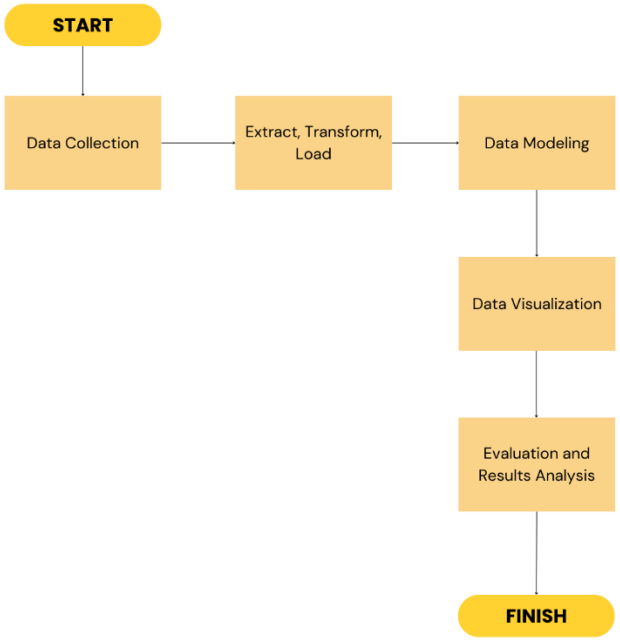

Figure 1. Flowchart of the research process

The flowchart in Figure 1 outlines the comprehensive research process, beginning with the collection of secondary data from official sources. Once the data are gathered, the process moves into the ETL phase, where data from two distinct periods (2020–2022 and 2023–2024) are extracted and merged into a unified dataset. During the transformation stage, the data undergo rigorous cleaning procedures including column alignment, duplicate removal, handling of missing values, and standardization of units and province labels to ensure consistency. After transformation, the cleaned data are loaded into Microsoft Power BI, where a robust data model

is constructed by defining relationships and setting appropriate data types, utilizing Power BI's in-memory OLAP capabilities for multidimensional analysis. Finally, the process culminates in the creation of interactive dashboards and visualizations, which enable users to filter and explore trends in corn production such as variations in harvested area, production volume, and productivity across different provinces and time periods, ultimately transforming raw data into actionable insights for informed decision-making.

Figure 2. ETL process

Figure 2 presents an expanded view of the ETL process. It starts with the extraction of data from two separate datasets: the Pre-2023 Dataset (2020–2022) and the Post-2023 Dataset (2023–2024). The process then moves to the transformation phase, where several key steps are performed. First, the merging of datasets is executed to consolidate all records into one unified dataset; next, column alignment is carried out so that common fields are uniform; then, duplicate rows are identified and removed; afterward, missing values are handled by setting them as NULL or zero for provinces not present in the earlier period; subsequently, unit standardization is performed to ensure consistency in measurements (for example, converting harvested area to hectares and production volume to tons); finally, province labels are standardized to ensure uniform naming across the entire dataset. The final step in this flowchart is the loading of the processed data into Microsoft Power BI, where it is further modeled for multidimensional analysis. Once the data are loaded into Power BI, a data model is established by defining relationships and setting data types. This step, known as data modeling, utilizes Power BI's in-memory OLAP capabilities to support multidimensional analysis across regions and time periods. Data visualization is the next stage, where interactive dashboards and visual representations are created. These visualizations allow users to filter and explore trends in corn production, revealing changes in harvested area, production volume, and productivity across various provinces and time periods.

	A	B	C	D	E	F	G	H	I	J	K	L	M	N	O	P
1	Province	Harvested Area (ha)					Productivity (ku/ha)					Production Volume (ton)				
2		2020	2021	2022	2023	2024	2020	2021	2022	2023	2024	2020	2021	2022	2023	2024
3	ACEH	11581,2	10289,99	12453,57	11728,37	10655,84	55,22	56,21	58,01	56,58	53,39	63950,8	57835,8	72241,64	66363,62	56894,99
4	NORTH SUMATRA	135334,4	153631,8	207756,8	211105,4	213549,1	57,87	62,29	62,93	63,63	64,2	783126,6	956938,9	1307477	1343291	1370961
5	WEST SUMATRA	65756,37	67159,49	84565,06	79630,77	83537,84	64,64	65,19	67,34	62,19	62,17	425025,4	437814,3	569450,4	495223,5	519323,8
6	RIAU	138,92	306,22	217,27	216,35	402,14	34,03	32,32	34,64	31,83	36,99	472,78	989,61	752,62	688,71	1487,59
7	JAMBI	1111	1665,97	1892,18	781,46	1976,09	68,45	58,34	55,37	60,46	63,91	7604,47	9719,01	10477,45	4724,77	12629,76
8	SOUTH SUMATRA	35073,88	51690,6	60187,49	46247,92	58343,76	60,37	61,23	76,48	61,55	62,68	211735,5	316505,6	460321,2	284643,3	365722,1
9	BENGKULU	4145,68	5983,25	10416,56	7900,85	10012,11	56,48	61,73	68,89	63,82	62,17	23415,58	36934,89	71755,99	50421,07	62243,19
10	LAMPUNG	156655	172108	223859,8	166215,3	169943,8	62,04	65,6	64,46	66,4	64,73	971957,4	1129112	1443096	1103640	1100082
11	BANGKA BELITUNG ISLANDS	28,73	97,31	62,8	23,25	2,59	44,09	35,85	41,08	47,87	44,94	126,66	348,85	257,95	111,3	11,64
12	RIAU ISLANDS	2,75	2,62	2,45	2,07	3,67	55,4	48,95	51,31	50,48	51,23	15,22	12,84	12,59	10,45	18,8
13	JAKARTA	-	-	-	-	-	-	-	-	-	-	-	-	-	-	-
14	WEST JAVA	59430,55	68213,91	95689,92	76901,39	81130,33	70,4	72,06	75,98	75,06	73,52	418401,7	491527,7	727067,6	577185,5	596508,8
15	CENTRAL JAVA	377065,2	340315,5	404493,4	371046,8	436330,9	60,44	62,56	59,94	58,6	59,29	2279146	2128959	2424371	2174484	2586896
16	YOGYAKARTA	31380,87	38391,14	42974,56	40056,38	37554,1	53,99	51,35	50,74	54,31	51,54	169430,7	197154,6	218046,4	217545,7	193564,3
17	EAST JAVA	722182,2	687502,7	817449,5	759060,9	735054	57,26	58,06	60,59	63,18	61,15	4134908	3991492	4952603	4795781	4494969
18	BANTEN	2945,5	1375,5	1250,54	1920,27	2215,42	69,09	68,29	76,79	74,82	62,27	20349,88	9393,64	9602,73	14367,12	13794,67
19	BALI	7927,98	10245,83	10316,71	9277,78	8454,47	44,14	48,92	51,57	50,55	55,36	34994,61	50117,54	53206,31	46901,81	46805,03
20	WEST NUSA TENGGARA	145562,6	156985,9	196064,9	179029,7	173191,3	59,12	64,92	72,52	71,55	66,6	860494,7	1019225	1421922	1281035	1153426
21	EAST NUSA TENGGARA	107094,9	111362,2	113624,5	101512,1	108531,3	23,85	25,62	25,85	25,8	26,68	255453	285344,6	293719,2	261854,9	289525,8

Figure 3. Screenshot of raw data

Figure 3 displays a screenshot of the consolidated raw data used in this study. The dataset comprises data for 38 provinces and includes fields such as year, province, harvested area, production volume, and productivity. The rows represent individual records for each province and year, while the columns correspond to the key variables mentioned. This visual confirmation ensures that the data have been accurately integrated and are ready for detailed analysis.

The evaluation and results analysis phase follows visualization, where the insights derived from the interactive dashboards are interpreted to inform conclusions and recommendations for

the agricultural sector. This systematic methodology, which integrates data consolidation within the transformation phase of the ETL process along with rigorous data modeling and advanced visualization in Power BI, ensures that the analysis is based on accurate, standardized data. The interactive dashboards developed enable users to explore trends in corn production across different regions and timeframes, ultimately supporting robust, data-driven decision-making in the agricultural sector.

Results and Discussions

Using Microsoft Power BI, this study thoroughly examined corn productivity data to generate interactive visualizations and dashboards that offer a comprehensive insight into regional trends. The analysis revealed notable patterns in harvested area, production volume, and productivity metrics, along with significant variations among provinces. These outcomes were discussed to assess their implications for agricultural policy and directions for future research.

Results

The data utilized in this study comprises annual corn productivity statistics, including harvested area, production volume, and productivity across various regions. It was obtained in Excel format from official sources. Preprocessing involved removing invalid or duplicate entries, normalizing formats, and grouping data by region and year. Data processed in the initial phase was then uploaded to Power BI, where visualizations were tailored to meet analytical needs. Graph types include bar charts to compare harvested areas, production volumes, and productivity across regions. An interactive dashboard was developed to integrate various visualizations and offer users the ability to filter data by year, region, or other categories.

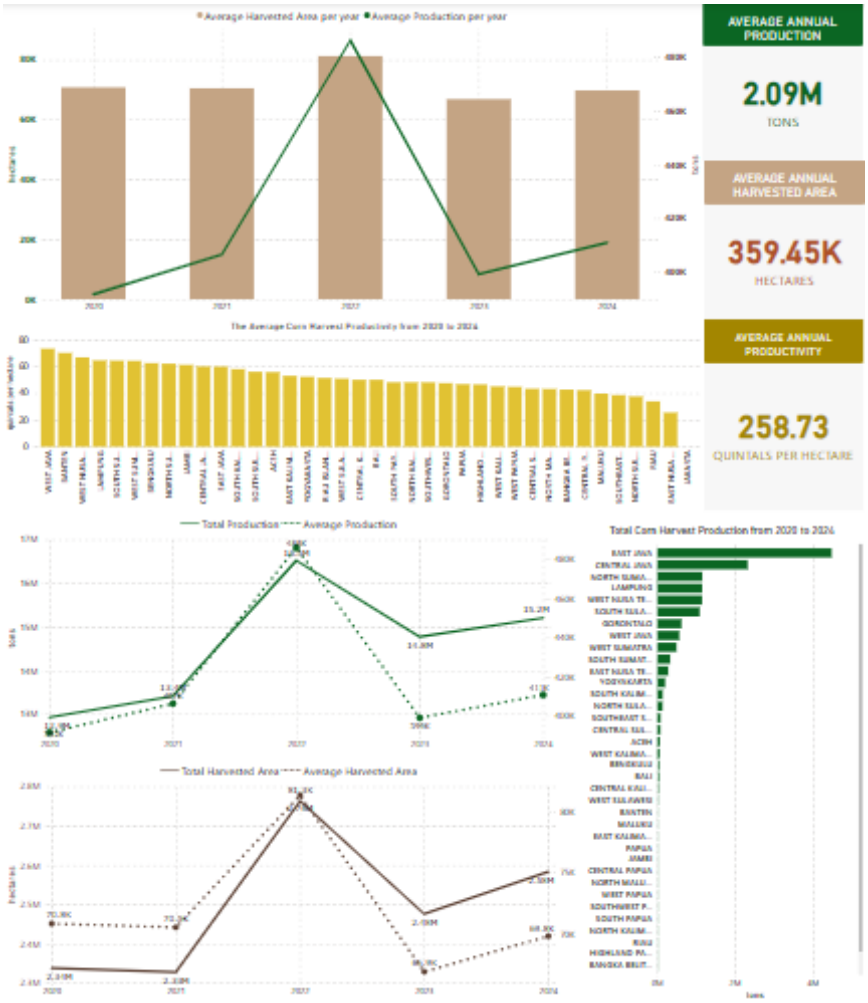

Figure 4. Corn productivity dashboard

The dashboard includes key visualizations such as the average harvested area per year, the average production volume per year, and the average productivity per hectare, all of which work together to provide critical insights into corn production trends. These visualizations offer a comprehensive overview of production metrics that are essential for understanding performance over time. Figure 4 illustrates this dashboard, which is designed to allow users to interact with the data dynamically, thereby enabling them to explore and analyze production trends across different regions and years in a highly intuitive manner.

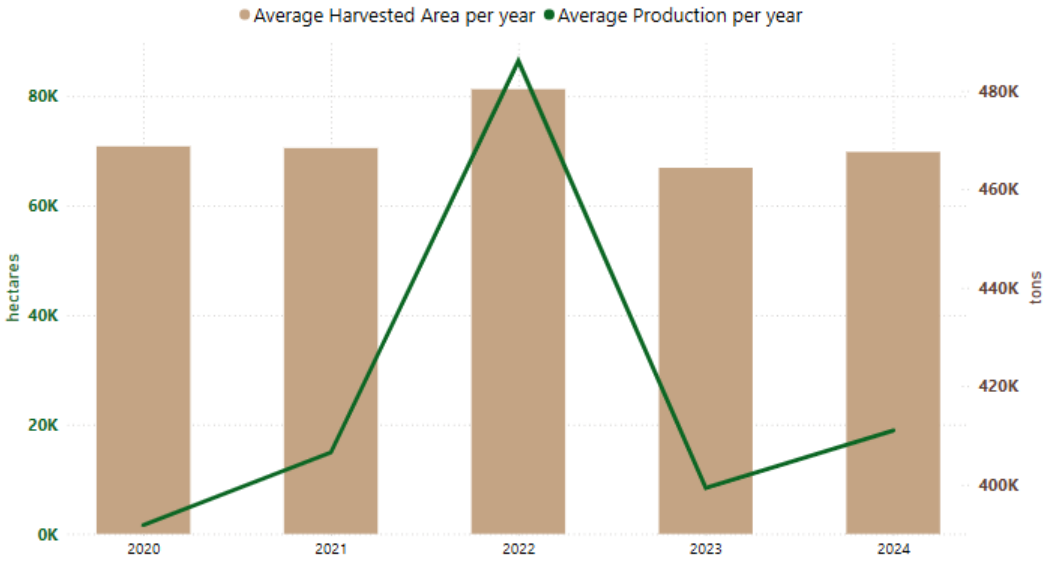

Figure 5. Average harvested area and production trends

Figure 5 delineates the temporal progression of the average harvested area and production volume from 2020 to 2024 and elucidates the inherent responsiveness of the corn production system to external perturbations. The peak observed in 2022, characterized by an 81.3 thousand-hectare harvested area and a production volume of 486 thousand tons, serves as a benchmark for optimal production conditions. In contrast, the marked decline in 2023 underscores the susceptibility of the production process to adverse meteorological events and supply chain disruptions, thereby highlighting systemic vulnerabilities. The subsequent, albeit incomplete, recovery in 2024 indicates that while remedial measures may ameliorate some adverse impacts, a latent fragility persists that warrants further intervention.

This visualization provides a critical empirical foundation for advocating enhanced risk management practices, infrastructural investments, and the integration of advanced forecasting technologies. Such measures are imperative for sustaining production stability and mitigating the effects of exogenous shocks, thereby reinforcing the strategic value of Business Intelligence tools in agricultural decision-making.

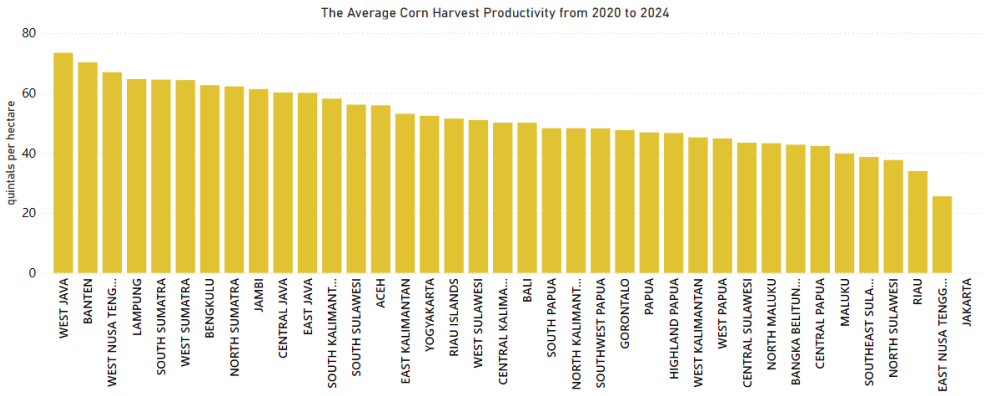

Figure 6. Average corn productivity per province

This chart clearly highlights significant productivity differences across provinces. For instance, West Java recorded the highest productivity, achieving an impressive level of around 80 quintals per hectare, while Jakarta registered no production data due to its completely urban landscape lacking any agricultural land. Additionally, East Nusa Tenggara exhibited the lowest productivity, with levels falling below 40 quintals per hectare. These variations not only reflect differing efficiencies in land use influenced by factors such as soil quality, access to modern technology, and overall resource management practices but also offer critical insights into regional disparities within the agricultural sector. Figure 6 provides a detailed visual comparison of these productivity levels, serving as an empirical foundation for further investigation into the effectiveness of localized agronomic practices and supporting targeted interventions aimed at optimizing production efficiency across diverse regions.

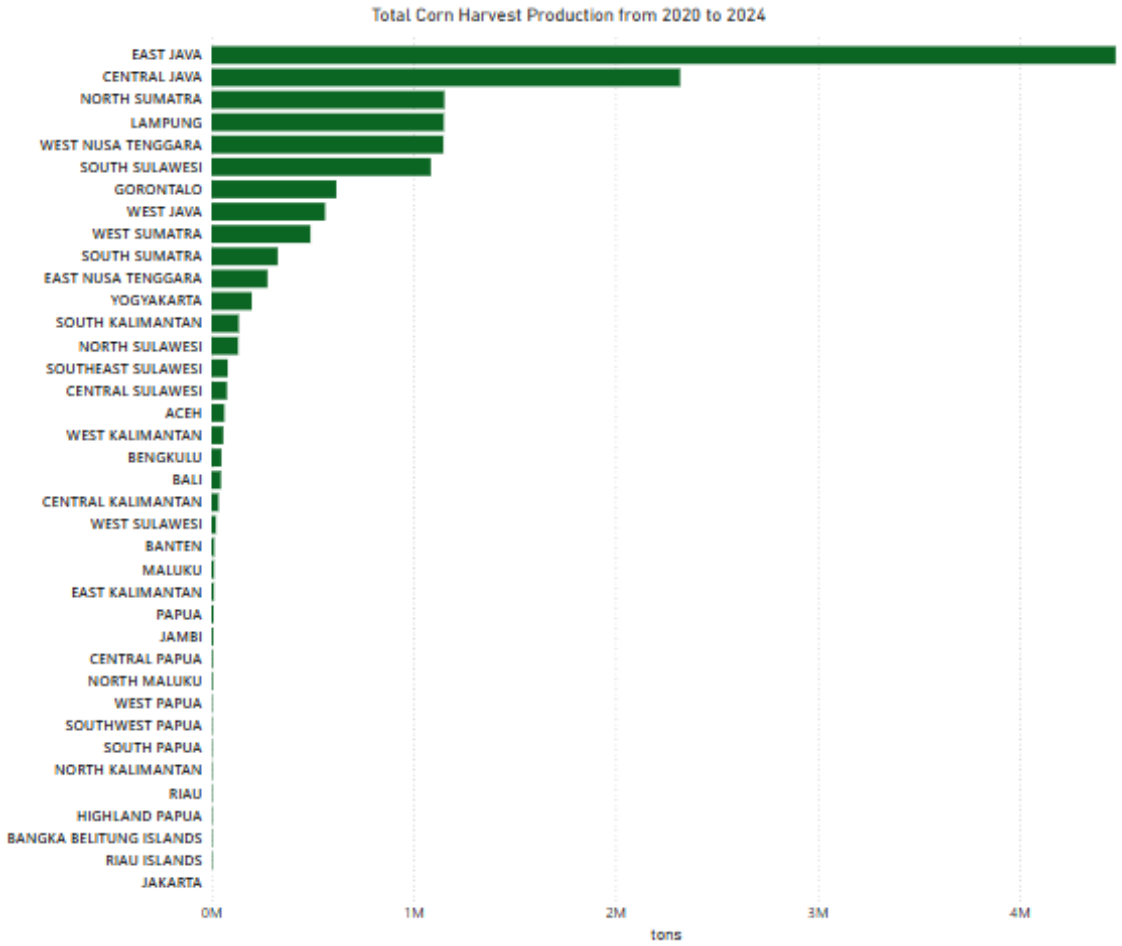

Figure 7. Corn production by province

Horizontal bar charts vividly illustrate the production capacities of various provinces over the period from 2020 to 2024. For instance, East Java led with a production exceeding 4 million tons, followed by significant contributions from Central Java and North Sumatra. In contrast, regions such as Jakarta showed no production data due to its urbanized landscape that lacks agricultural land, and several provinces in Papua (including Southwest Papua, South Papua, Central Papua, and Highland Papua) have missing data for 2020–2022 as they were newly established administrative regions. These visualizations provide not only a clear differentiation of regional production capacities but also serve as a critical indicator for identifying areas that may benefit from focused developmental strategies. By pinpointing these disparities, the chart offers valuable insights into where infrastructural investments and tailored policy interventions could bolster agricultural development and enhance regional productivity. Figure 7 , therefore, acts as a foundational reference for both researchers and policymakers aiming to understand and address the spatial imbalances in corn production across the nation.

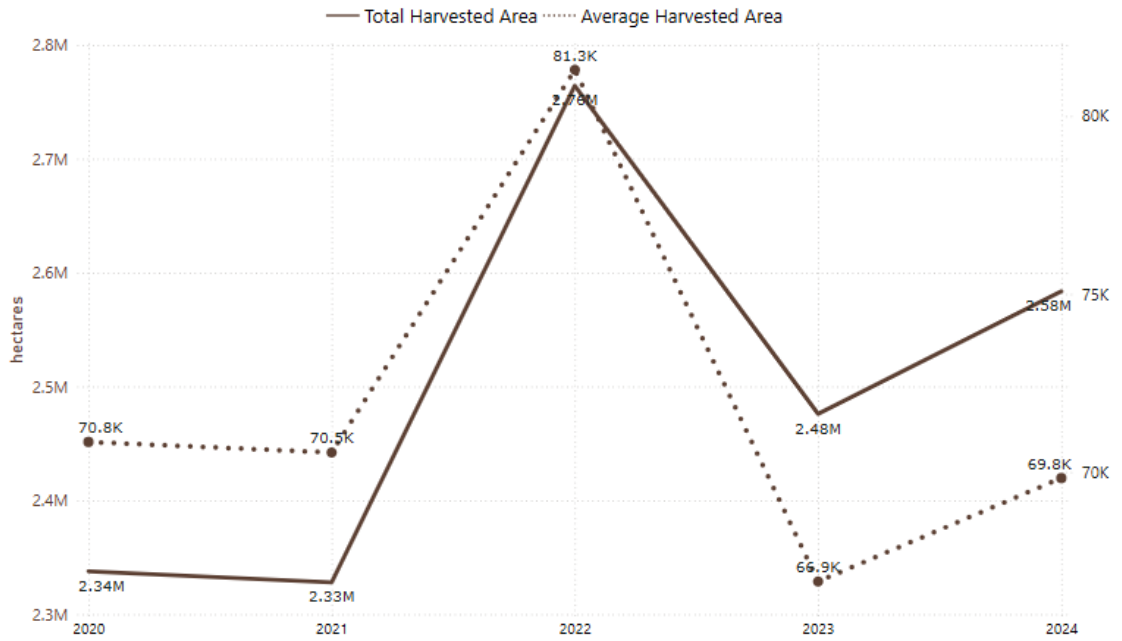

Figure 8. Annual harvested area trends

Annual trends in harvested area from 2020 to 2024 exhibit fluctuations driven by factors such as climate change and land allocation policies. In 2022, the harvested area peaked at 2.81 million hectares, followed by a decline to 2.48 million hectares in 2023, and a slight recovery in 2024. This pattern is significant because it reflects how environmental conditions and policy decisions directly affect agricultural land use. The decline in 2023 may indicate the impact of adverse weather conditions or shifts in land management practices, suggesting vulnerabilities in the current agricultural framework. Moreover, the partial recovery in 2024 implies that while some corrective measures may have been effective, the system has not yet returned to its previous optimal state. Figure 8 offers a clear view of these temporal trends and anomalies, serving as a vital empirical basis for further investigation into the dynamics between environmental factors, land policy, and agricultural productivity.

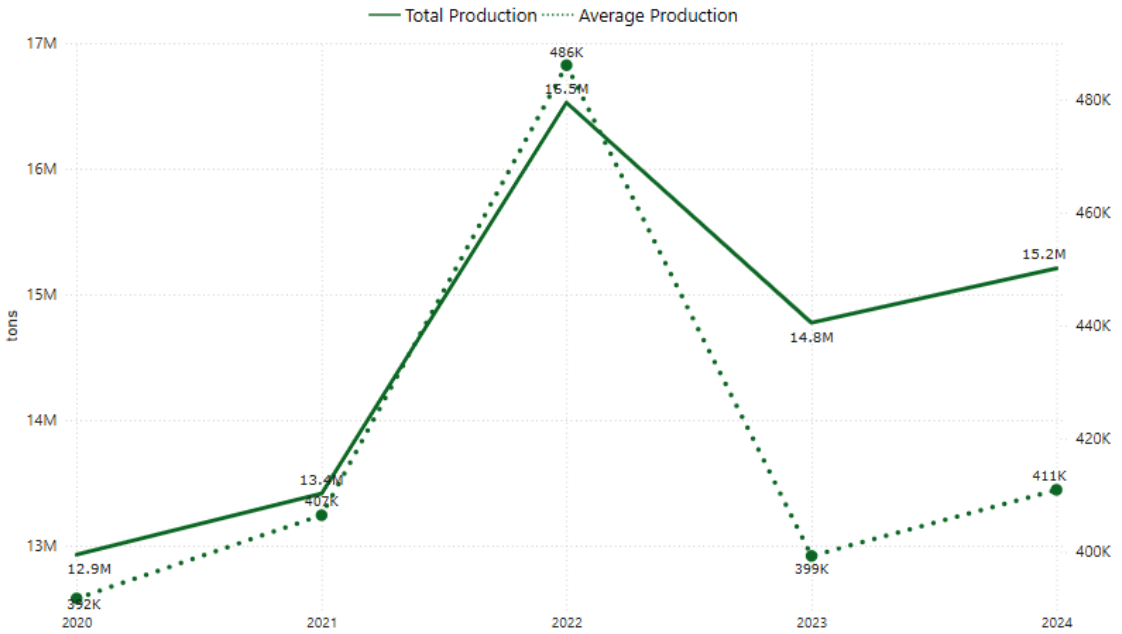

Figure 9. Annual corn production trends

Production trends mirror those observed in the harvested area, with 2022 achieving the highest output at 15.5 million tons, a decline to 14.8 million tons in 2023, and a partial recovery to 15.2 million tons in 2024. This pattern is significant because it underscores the direct influence of external factors such as climate variability, market dynamics, and infrastructural constraints on corn yields. The drop in production in 2023 may reflect the adverse effects of unfavorable weather and supply chain disruptions, while the recovery in 2024 suggests that mitigation strategies and adaptive practices are beginning to yield positive results. Figure 9 provides a visual representation of these fluctuations and serves as an empirical foundation for analyzing the resilience of corn production systems, highlighting the need for continuous monitoring and targeted policy interventions to stabilize yield performance over time.

Figure 10. Summary metrics

A scorecard in Figure 10 summarizes key performance indicators such as average production (2.09 million tons per year), average productivity (258.73 quintals per hectare), and average harvested area (359.45 thousand hectares per year). These aggregate metrics not only provide a snapshot of overall corn production performance but also offer a robust framework for benchmarking agricultural outcomes. The integration of these indicators allows policymakers to evaluate production efficiency and identify critical areas for improvement. Furthermore, the summary metrics serve as a basis for comparing historical trends and projecting future performance under varying policy scenarios and environmental conditions. This empirical foundation is essential for designing targeted interventions and optimizing resource allocation within the agricultural sector.

Discussions

The results highlight significant trends and disparities in corn productivity across regions and years, offering insights into various factors that affect production performance. The peak in harvested area and production volume in 2022 likely reflects favorable conditions, including improved weather and government interventions, whereas the subsequent decline in 2023 underscores the vulnerabilities of agricultural production to external disruptions such as climate change and supply chain issues [5]. The partial recovery in 2024 suggests that corrective measures have been effective, yet it emphasizes the need for sustained efforts to maintain stability in production levels.

Regional disparities in productivity are evident; for example, West Java's high productivity points to the benefits of advanced agricultural technologies, robust infrastructure, and efficient resource management [4], [6]. In contrast, areas with lower productivity encounter challenges such as poor soil quality, limited access to modern farming methods, and insufficient infrastructure. While Jakarta's lack of corn production is an anticipated outcome due to its predominantly urban landscape and limited agricultural zones, this phenomenon warrants a deeper exploration of urbanization's broader implications on regional agricultural dynamics. Urban expansion often precipitates significant changes in land use, influencing not only the availability of arable land but also altering food supply chains and economic relationships between urban centers and their rural peripheries. For instance, Jakarta's case can be seen as a microcosm of how rapid urban development may lead to increased dependency on food production from

surrounding regions, potentially creating vulnerabilities in local food security and contributing to socio-economic disparities. Further research should investigate these urban-rural linkages, examining how shifts in demographic patterns, land use policies, and infrastructure development collectively impact agricultural productivity and regional sustainability. Such insights would provide a more nuanced understanding of how urbanization, while expected to reduce local production, also plays a pivotal role in shaping broader agricultural and economic landscapes. Similarly, the lack of data for Papua, Southwest Papua, South Papua, Central Papua, and Highland Papua during 2020–2022 is attributed to their recent administrative establishment rather than a failure in production, underscoring the impact of evolving regional boundaries on data reporting.

Integrating these findings with established agricultural theories reinforces the importance of adopting precision agriculture techniques and data-driven policymaking. The use of Power BI in this study demonstrates how modern Business Intelligence tools can transform raw data into actionable insights, thereby supporting more efficient decision-making. These insights suggest that targeted policies are needed to address regional disparities, improve data collection in newly established regions, and prioritize technological advancements. Future research should explore the long-term impacts of these interventions and expand the application of data visualization tools to additional crops and regions, further contributing to sustainable agricultural development across Indonesia [7], [8], [14].

Conclusion

This study underscores the transformative role of Business Intelligence in addressing Indonesia's agricultural challenges, particularly in analyzing corn production trends and regional disparities between 2020 and 2024. Using Microsoft Power BI, the research revealed critical insights into production volatility linked to climate disruptions, such as a 4.5% decline in 2023, and stark productivity contrasts between high-performing agrarian regions like West Java, which achieved 80 quintals per hectare, and non-agrarian zones such as Jakarta. However, the study has limitations, including data gaps in newly established provinces such as Southwest Papua and reliance on a single BI platform, which may affect the generalizability of findings. Additionally, the simplification of external factors like interactions between climate and market dynamics may underestimate systemic risks. Future research should expand temporal and spatial granularity by integrating IoT and satellite data, employ machine learning to model compound risks such as simultaneous drought and inflation, and compare BI tools including Power BI and Tableau for agricultural applications. Exploring urban farming models in densely populated regions and tracking policy impacts through real-time BI dashboards could further bridge rural-urban divides. By addressing these limitations, interdisciplinary collaborations can advance equitable, data-driven agricultural governance, ensuring resilience across Indonesia's diverse landscapes.

Acknowledgments

We extend our heartfelt gratitude to Universitas Semarang for their unwavering support, which has been instrumental in facilitating this research. Their commitment to fostering academic innovation has enabled us to delve deeply into the intersection of technology and financial behavior. We also wish to express our sincere appreciation to P3M Politeknik Negeri Bali for providing an excellent platform to publish this journal. The opportunity to share our findings through such a reputable publication is greatly valued. The collective support from these institutions has been pivotal in making this study possible and advancing knowledge in the field of financial technology and risk assessment. We are truly grateful for their collaboration and encouragement.

References

[1] A. Hudoyo and I. Nurmayasari, "Peningkatan produktivitas jagung di Indonesia," *Indonesian Journal of Socio Economics*, vol. 1, no. 2, pp. 102-108, 2020.

[2] F. Melia, F. M. Aldian, M. S. F. Pahlevi, R. N. I. Risqullah, and S. Oktaffiani, "Peran pemerintah dalam meningkatkan volume ekspor jagung," *Jurnal Economina*, vol. 2, no. 1, pp. 269-284, 2023.

[3] R. Yunita, "Peran Dinas Ketahanan Pangan Perikanan Tanaman Pangan dan Hortikultura dalam Mengendalikan Inflasi Daerah di Kabupaten Tabalong," *JAPB*, vol. 7, no. 1, pp. 887-902, 2024.
[4] M. D. Riyanda and S. Suyanto, "Implementasi Business Intelligence Pada Analisis Perkembangan Hasil Pertanian Provinsi Sumatera Selatan," *Journal of Computer and Information Systems Ampera*, vol. 1, no. 3, pp. 174-184, 2020.
[5] R. Vroegindewey and J. Hodbod, "Resilience of agricultural value chains in developing country contexts: A framework and assessment approach," *Sustainability*, vol. 10, no. 4, Mar. 2018.
[6] G. Vico, D. Mijic, and R. Bodiroga, "Business Intelligence in Agriculture–A Practical Approach," *AGRI BASE*, 2019.
[7] J. R. Sunkara, S. R. Bauskar, C. R. Madhavaram, E. P. Galla, and H. K. Gollangi, "Data-Driven Management: The Impact of Visualization Tools on Business Performance," *International Journal of Management (IJM)*, vol. 12, no. 3, pp. 1290-1298, 2021.
[8] S. Bussa, "Enhancing BI Tools for Improved Data Visualization and Insights," *International Journal of Computer Science and Mobile Computing*, vol. 12, no. 2, pp. 70-92, 2023.
[9] A. Maulana and D. A. Wulandari, "Business Intelligence Implementation to Analyze Perfect Store Data Using the OLAP Method," *SinkrOn*, vol. 3, no. 2, p. 97, Mar. 2019.
[10] L. M. Aini, "Penentuan provinsi-provinsi terbaik dalam produksi jagung nasional melalui analisis kuadran atas variable produksi dan produktivitas per satuan luas lahan," *Jurnal Ekonomi Pertanian dan Agribisnis*, vol. 3, no. 4, pp. 751-760, 2019.
[11] V. M. Ngo, N. A. Le-Khac, and M. Kechadi, "An efficient data warehouse for crop yield prediction," *arXiv preprint arXiv:1807.00035*, 2018.
[12] R. Wijaya and B. Pudjoatmodjo, "Penerapan Extraction-Transformation-Loading (ETL) Dalam Data Warehouse (Studi Kasus : Departemen Pertanian)," *Jurnal Nasional Pendidikan Teknik Informatika (JANAPATI)*, vol. 5, no. 2, 2016.
[13] E. O. Eboigbe, O. A. Farayola, F. O. Olatoye, O. C. Nnabugwu, and C. Daraojimba, "Business intelligence transformation through AI and data analytics," *Engineering Science & Technology Journal*, vol. 4, no. 5, pp. 285-307, 2023.
[14] K. G. Sanabia-Lizarraga, B. Carballo-Mendívil, A. Arellano-González, and A. Bueno-Solano, "Business Intelligence for Agricultural Foreign Trade: Design and Application of Power BI Dashboard," *Sustainability*, vol. 16, no. 21, Nov. 2024.
[15] N. Chergui and M. T. Kechadi, "Data analytics for crop management: a big data view," *J Big Data*, vol. 9, no. 1, Dec. 2022.

Matrix: Jurnal Manajemen Teknologi dan Informatika
Volume 15 Issue 1 Year 2025 Pages 32-39
DOI: http://dx.doi.org/10.31940/matrix.v15i1.32-39
URL: http://ojs2.pnb.ac.id/index.php/matrix

Development of a hybrid model for website functional evaluation based on ISO/IEC 25010 and SERVQUAL

Ardiva Putri Tava Prameswari [1]*, Muhammad Yusril Helmi Setyawan [2]

[1,2] *Informatics Engineering, Universitas Logistik dan Bisnis Internasional, Indonesia*

*Corresponding Author: *ardiva.diva30@gmail.com*

Abstract: This study developed a hybrid model based on ISO/IEC 25010 and SERVQUAL to evaluate website quality holistically by combining technical dimensions and user perceptions. ISO / IEC 25010 is an international standard for evaluating the quality of software, including websites, based on technical characteristics such as Functional Suitability, Usability, Reliability, and Security. SERVQUAL, on the other hand, is used to measure quality based on user perception through five main dimensions: Tangibles, Reliability, Responsiveness, Assurance, and Empathy. This study aims to identify the gaps between user expectations and the reality of website performance by using both frameworks. The research method combines quantitative and qualitative approaches, with user surveys and direct observation as data collection tools. The results of the analysis showed that most website quality dimensions, such as Functional Suitability, Usability, Reliability, Responsiveness, and Security, were in the category of "very adequate," with a relatively small gap between actual and expected scores. This study also tested the validity and reliability of constructs using convergent and discriminant analysis, as well as hypothesis testing to identify significant influences between variables. Hypothesis test results show that usability, reliability, and satisfaction variables have a significant influence on user experience. At the same time, factors such as functional fit and physical appearance do not directly affect user experience. This hybrid model provides theoretical contributions by enriching the literature on website Quality Evaluation and practical contributions by providing guidance for website managers to improve the quality of their services based on the identification of gaps between actual performance and user expectations.

Keywords: hybrid model, ISO/IEC 25010, SERVQUAL, website quality evaluation

History Article: Submitted 24January 2025 | Revised 30 March 2025 | Accepted 22 April 2025

How to Cite: A. P. T. Prameswari and M. Y. H. Setyawan, "Development of a hybrid model for website functional evaluation based on ISO/IEC 25010 and SERVQUAL", *Matrix : Jurnal Manajemen Teknologi dan Informatika*, vol. 15, no. 1, pp. 32–39, 2025. doi.org/10.31940/matrix.v15i1.32-39.

Introduction

In the digital era, websites have become essential elements for various organizations, whether in business, education, or public service sectors. A website's role is not only limited to providing information but also as a service provider that directly interacts with users. Therefore, maintaining website quality is a crucial step to ensure optimal user experience, reliable functionality, and stable system performance [1]. As user expectations increase, website quality evaluation has become increasingly complex. Many traditional evaluation methods have not been able to combine technical performance and user perception thoroughly. This creates a need for a more integrated and holistic evaluation approach, which not only assesses technical aspects but also considers user satisfaction and expectations.

This research aims to address this challenge by developing a hybrid evaluation model that combines two main approaches, namely technical standards and service perceptions. This model is expected to provide a more comprehensive picture of website quality and identify gaps between actual performance and user expectations [2]. Specifically, the objectives of this research are develop a hybrid evaluation model based on ISO/IEC 25010 and SERVQUAL to improve the effectiveness of website functional quality assessment, identify the most influential dimensions and indicators on website quality and validate the model through factor analysis and hypothesis testing. This research also tests the model on an internship website that is used as a connecting

platform between job seekers and industries, thus directly contributing to the improvement of digital service quality.

Through this approach, the research is expected to make a theoretical contribution to the development of website quality evaluation methods, as well as a practical contribution in providing guidance for website managers in designing service improvement strategies based on data and user perceptions [3]. This study applies the hybrid evaluation model to analyze an apprenticeship website that provides career-related services to students and job seekers. The website functions as a bridge between industries seeking skilled professionals and individuals looking for employment opportunities [4]. By implementing the hybrid model, this study aims to demonstrate its applicability in assessing website quality and improving user satisfaction.

This research contributes to two main aspects. Theoretically, it enriches the literature on website quality evaluation by proposing a hybrid model that integrates technical and user experience perspectives. Practically, it offers valuable insights for website managers and developers in optimizing website performance based on a structured and user-centred evaluation framework [5]. By identifying and addressing gaps between actual performance and user expectations, website managers can implement targeted improvements to enhance overall service quality. Ultimately, this study provides a novel contribution to website evaluation methodologies, offering a systematic approach to improving digital service platforms.

Methodology

This research employs a mixed method approach, combining quantitative and qualitative methods to evaluate website quality comprehensively. The study aims to identify gaps between user expectations and actual website performance by integrating two main frameworks: ISO/IEC 25010 and SERVQUAL. This hybrid approach allows for a holistic assessment of both the software's technical quality and the user experience [1].

The quantitative approach involves evaluating website quality based on the dimensions of ISO/IEC 25010 and SERVQUAL, forming a hybrid model that provides a comprehensive analysis of technical and service quality aspects [2]. The integration of these frameworks is illustrated in Figure 1, which demonstrates the relationship between technical quality dimensions and service quality aspects, highlighting how both frameworks work together to deliver a complete website evaluation.

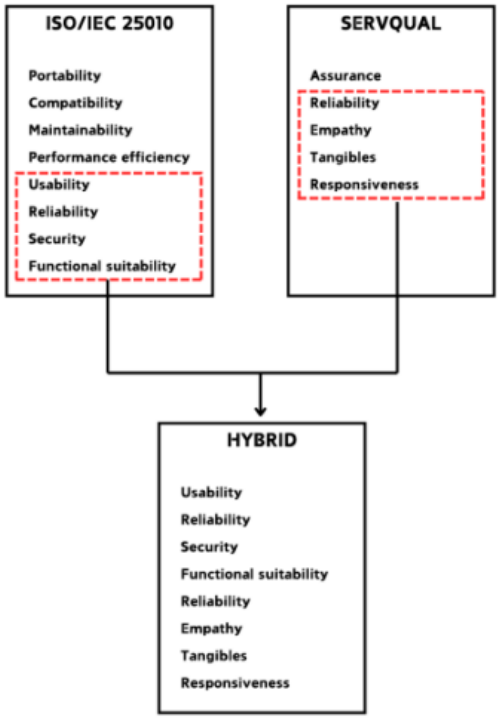

Figure 1. Hybrid model

Data Collection and Analysis

The website evaluation was conducted through user surveys and direct observation. The surveys collected user perceptions regarding various website quality dimensions, while direct observation assessed technical elements such as interface design, response speed, and security features [6]. Performance efficiency testing was conducted using Google's PageSpeed Insights tool, where website efficiency was categorized into three levels based on performance scores, as shown in Table 1.

Table 1. Performance score categories

Eligibility Criteria	Score Percentage (%)
Slow	0% - 49%
Average	50%-89%
Fast	90%-100%

A gap analysis was applied to compare website performance against user expectations, identifying discrepancies between anticipated and actual service quality. The interpretation of performance scores was based on SERVQUAL and ISO/IEC 25010, classifying website quality into five categories, as detailed in Table 2 [7].

Table 2. Quality score interpretation

Eligibility Criteria	Score Percentage (%)
Very Inadequate	0% - 20%
Inadequate	21% - 40%
Sufficient	41% - 60%
Adequate	61% - 80%
Very Adequate	81% - 100%

The study involved a sample of 650 respondents obtained through survey distribution. To analyze the collected data, Partial Least Squares Structural Equation Modeling (PLS-SEM) was employed to identify key dimensions affecting website quality. By integrating ISO/IEC 25010 and SERVQUAL, along with gap analysis and PLS-SEM, this research provides a comprehensive evaluation framework that serves as a basis for further website quality improvement and development.

Results and Discussions

Results

After distributing the questionnaire, the collected responses were processed for analysis. This process includes analysis of respondents' answers based on a predetermined assessment scale. Previously, in the questionnaire there were 5 answer choices, namely Strongly Agree (SS), Agree (S), Neutral (KS), Disagree (TS), and Strongly Disagree (STS). These answer choices are designed to measure the respondent's level of agreement or perception of each indicator related to the question in each dimension studied [8].

The next step is to analyze the respondent's profile which contributes to their perception of the system under study. This respondent profile is important for understanding the demographic context that may influence assessment results. Table 3 shows the profile of respondents based on age and profession, which shows that the majority of respondents came from school and college students.

Table 3. Respondent profile

Information	Frequency	%
Age		
15-19	237	36
20-25	199	30
26-40	214	32
Profession		
High school student	237	36
College student	199	30
Lecturer/Teacher	214	32

This demographic context is important in interpreting how perceptions of website quality may vary based on age and educational background. Using ISO/IEC 25010 dimensions combined with SERVQUAL, the average actual scores and expectations were measured. The gap score (difference between actual and expected) indicates the performance shortfall [9].

Table 4. Matrix assessment

Dimensions	Current Score (ISO/IEC 25010)	Expectation Score	Gap	Eligibility Criteria
Functional Suitability	4.07	5	0.93	Very Adequate
Usability	4.09	5	0.91	Very Adequate
Reliability	4.08	5	0.92	Very Adequate
Responsiveness	4.13	5	0.87	Very Adequate
Security	4.06	5	0.94	Very Adequate
Tangibles	4.04	5	0.96	Adequate
Empathy	4.09	5	0.91	Very Adequate
User Experience	4.07	5	0.93	Very Adequate

All dimensions achieved actual scores above 4.00, with responsiveness scoring the highest (4.13) and tangibles scoring the lowest (4.04). Despite the gaps, most dimensions fall into the "Very Adequate" category (≥81%), except for Tangibles, which is classified as "Adequate" (80%).

To confirm the validity of the instrument, convergent and discriminant validity tests were performed.

a. Convergent Validity: All indicators had a loading factor > 0.50. For example, E1 (0.742), F1 (0.770), and R1 (0.694).
b. Discriminant Validity: Each indicator correlated higher with its construct than with other constructs, satisfying the discriminant validity criteria.

Table 5. Reliability test

Construct	Cronbach's Alpha	Composite Reliability
F	0.532	0.755
R	0.471	0.733
S	0.629	0.780
UE	0.588	0.755

The results of the reliability test show that most of the constructs have a Cronbach's Alpha value greater than 0.50, although there are several constructs that are close to the minimum limit, such as the R construct (0.471). However, Composite Reliability for all constructs is above 0.70, which indicates good reliability, with the examples of constructs F and UE each having a Composite Reliability value of 0.755.

To evaluate the extent to which the independent variables in the model are able to explain the dependent variable, an R-Square analysis was carried out. The results of this analysis are

presented in Table 6, which provides an overview of the strength of the relationship between variables in the research model.

Table 6. R-Square results

Dependent Variable	R^2 Value
Satisfaction (S)	0.660
Intention (IN)	0.544
User Experience (UE)	0.880

The R-Square value for the variables S (0.660), IN (0.544), and UE (0.880) shows that this model can explain the variance of the dependent variable quite well. The UE variable has the highest R-Square value, namely 0.880, which shows that the independent variables in this model greatly influence the user experience.

After knowing the extent to which the independent variable is able to explain the dependent variable through the R-Square value, the next step is to test the causal relationship between the variables in the model. Hypothesis testing is carried out to identify the significant influence of each independent variable on the dependent variable, as summarized in the following results [10]:

Table 7. Hypothesis testing

Relationship	Coefficient	T-Statistic	P-Value	Significance
F → Usability	0.759	15.983	0.000	Strong positive effect
R → Satisfaction	0.813	55.784	0.000	Strong positive effect
U → User Experience	0.870	29.802	0.000	Very strong positive effect
T → User Experience	0.157	4.687	0.000	Moderate positive effect

Based on the results of hypothesis testing in Table 7, most of the relationships between variables show significance, with a p-value <0.05. Significant relationships include F → U (T = 15.983, P = 0.000), which indicates that functional suitability has a strong influence on ease of use, as well as U → UE (T = 29.802, P = 0.000), which indicates that usability has a large influence on user experience. In addition, the variable R → S (T = 55.784, P = 0.000) shows that reliability significantly influences user satisfaction, while RS → UE (T = 3.799, P = 0.000) and T → UE (T = 4.687, P = 0.000) also has a significant impact on user experience. However, some relationships were not significant, such as F → UE (T = 0.856, P = 0.392) and T → U (T = 0.550, P = 0.583), indicating that functional suitability and physical appearance do not directly influence user experience or convenience. This confirms that usability, reliability and satisfaction factors are more dominant in influencing user experience.

Discussions

The results of the study reveal that most of the dimensions evaluated using the ISO/IEC 25010 model were considered as "Very Adequate," with a significant gap between the actual and expected scores for certain dimensions, particularly Tangibles. The findings show that respondents perceive the system as reliable and usable [11]. However, there is a notable need for improvements in areas related to the tangible elements of the system, such as the interface design and aesthetics. This aligns with the findings from Priya and Khalil (2020), who emphasized the importance of software interface design in ensuring the overall quality of a web-based portal. Their study, which used the ISO/IEC 25010 model, also highlighted the significant role of user

perception in determining the adequacy of system elements such as functionality and usability [12].

Moreover, the reliability analysis, which shows satisfactory Cronbach's Alpha and Composite Reliability values, supports the reliability of the constructs being measured. However, some constructs, such as "Reliability" and "Responsiveness," had lower Cronbach's Alpha values, indicating slight inconsistencies in the internal consistency. Nevertheless, their high Composite Reliability values suggest that these constructs remain reliable. This finding corroborates Laurence and Candiwan's (2020) research, which demonstrated that while internal consistency might vary, the overall reliability of constructs could still be considered robust when Composite Reliability scores exceed the threshold of 0.70 [13].

The R-Square analysis, particularly the high value for User Experience (UE) (0.880), suggests that the independent variables in the study usability, reliability, and responsiveness have a strong impact on user experience, further supported by hypothesis testing results. These results align with previous research by Gelgel et al. (2024), which found that the user experience significantly influences the perceived quality of tourism communication platforms, similar to the way usability and responsiveness affect the user experience in software systems. Their study, which focused on local wisdom-based communication, reinforced the idea that the quality of interaction directly influences user satisfaction [14].

Overall, the study's findings highlight that while the software quality dimensions of functionality, usability, and reliability were perceived as very adequate, tangible elements, such as the interface design, require significant improvement to meet user expectations. This suggests a need for further enhancements in design aesthetics and system responsiveness to improve overall user satisfaction, as emphasized by Priya and Khalil (2020) and Laurence and Candiwan (2020) [15].

The implications of this study extend to both theory and practice. For theory, the findings contribute to understanding the role of ISO/IEC 25010 in assessing software quality from a user perspective. For practice, developers should prioritize improving the design and tangible elements of software systems, as these factors significantly impact user satisfaction. Future research could explore how specific design improvements, such as the implementation of more intuitive user interfaces, might reduce the gap between expected and actual user perceptions.

This study also contributes to the development of software quality models by integrating user experience insights and providing empirical evidence on the importance of specific dimensions, such as usability and reliability, in driving user satisfaction and system acceptance.

Conclusion

This research succeeded in developing a hybrid model based on ISO/IEC 25010 and SERVQUAL to evaluate website quality holistically by combining technical dimensions and user perception. The analysis results show that most of the website quality dimensions, such as Functional Suitability, Usability, Reliability, Responsiveness, and Security are in the "Very Adequate" category, with a relatively small gap between actual and expected scores. Construct validity and reliability have also been tested, showing sufficient results to support further analysis. The results of hypothesis testing reveal that the variables usability, reliability, and satisfaction have a significant influence on user experience, whereas functional suitability and physical appearance do not directly influence it.

This model provides a theoretical contribution by enriching the website quality evaluation literature and providing a practical contribution by guiding website managers to improve service quality based on identifying gaps between actual performance and user expectations. Therefore, it is recommended that website developers prioritize improving usability and reliability aspects that significantly affect user experience. Website managers should also conduct regular assessments using the hybrid model to monitor performance gaps over time. For future researchers, it is advisable to apply this model in various domains or platforms to validate its flexibility and scalability across different website types. Thus, this hybrid approach can be an effective framework for designing a more focused and efficient website quality improvement strategy.

Acknowledgments

This research was completed with the support and collaboration of various individuals and organizations. First and foremost, we express our deepest gratitude to University of Logistic and Business International for providing the necessary resources and guidance throughout this study. We want to extend our sincere appreciation to our research supervisor, Mr. Yusril Helmi, for his invaluable feedback, encouragement, and expertise, which greatly enhanced the quality of this research. A special thanks to all the participants who contributed their time and insights through surveys and interviews, as their input was essential for the analysis and findings presented in this paper. Lastly, we acknowledge the support of our families and friends for their patience, motivation, and understanding during the entire research process. This work would not have been possible without the collaborative efforts and shared dedication of all involved.

References

[1] S. R. N. A. Hasanah and L. Atikah, "Functional Suitability Measurement Based on ISO/IEC 25010 for e-Commerce Website," *7th Int. Conf. Inf. Technol. Comput. Electr. Eng. ICITACEE 2020 - Proc.*, pp. 70–75, 2020, doi: 10.1109/ICITACEE50144.2020.9239194.

[2] D. A. S. and E. Sulistiyani, "Evaluation of Information Quality Using ISO/IEC 25010:2011 (Case Research: Menu Harianku Application)," *Int. J. Innov. Enterp. Syst*, vol. 6, no. 2, pp. 143–156, 2022.

[3] M. L. et Al, "Análisis del modelo de calidad en uso y la sostenibilidad aplicando la Norma ISO/IEC 25010 Analysis of the Quality in Use and Greenability with the ISO / IEC 25010 Standard," *Iber. Conf. Inf. Syst. Technol.*, no. Juni, pp. 24–27, 2020.

[4] O. H. K. Moumane and A. Idri, F. El Aouni, J. Laghnimi, N. C. Benabdellah, "ISO/IEC 25010-based Quality Evaluation of Three Mobile Applications for Reproductive Health Services in Morocco," *Clin. Exp. Obs. Gynecol.*, vol. 51, no. 4, 2024, doi: 10.31083/j.ceog5104088.

[5] I. S. and N. Nursaeni, "Implementasi Asesmen Instrumen Kualitas Menggunakan Model Kualitas ISO/IEC 25010 dan ISO/IEC 9126 Pada Sistem Informasi Akademik SIPAKATAU Berbasis Pengalaman Pengguna," *Inspir. J. Teknol. Inf. dan Komun*, vol. 12, no. 1, p. 96, 2022.

[6] E. S. F. Nurunnisa and M. L. Hamzah, Angraini, "Analyzing the Quality of Web-Based Scholarship Information System Using ISO/IEC 25010 Standard," *Int. Conf. Circuit, Syst. Commun. ICCSC*, 2024, doi: 10.1109/ICCSC62074.2024.10617354.

[7] A. A. P. M. L. Hamzah and A. Yeskermessuly, Y. Oktinadila, Nazaruddin, "Measurement of Usability, Information Quality, Service Information Quality on News Portals Website using Important Performance Analysis," *J. Logist. Informatics Serv. Sci*, vol. 10, no. 4, pp. 35–46, 2023, doi: 10.33168/JLISS.2023.0403.

[8] H. P. W. and M. Kholil, "Analysis of Quality Village Portal Based on Web Using Content Management System in Iso/Iec 25010 Product Quality Model," *J. Teknol. dan Ter. Bisnis*, vol. 3, no. 1, pp. 35–39, 2020.

[9] S. L. and Candiwan, "The Role of Trust Toward Continuance Usage Intention: of Mobile Payment with Gender as Moderation," *E-Bisnis J. Ilm. Ekon. dan Bisnis,* vol. 13, no. 1, pp. 64–73, 2020, doi: 10.51903/e-bisnis.v13i1.170.

[10] A. I. A. P. W. S. K. D. Gelgel, I. G. A. Wima, "Rangrang : Pesona Nusa Penida Sebagai Simbol Komunikasi Pariwisata Berkelanjutan Berbasis Kearifan Lokal (Studi kasus : IKM Ngurah Gallery, Desa Tanglad, Nusa Penida, Klungkung, Provinsi Bali)," *J. Pesona Pariwisata*, vol. 3, no. 1, pp. 1–6, 2024, doi: 10.33005/peta.v3i1.58.

[11] M. Huda, *Writing Modern Digital Books: An Anthology of Journals Writing and Publishing E-books*. Jakarta, Indonesia: Bitread Publishing, 2021.

[12] R. Mission, "Online Support Management System for University of Antique," *J. Innov. Technol. Converg*, vol. 2, no. 2, pp. 39–52, 2020.

[13] H. D. B. S. A. Ardana and F. Sukmana, "Evaluasi Kualitas User Interface Pada Situs Website Booking System 'Kantoor' Menggunakan ISO/IEC 25010 Dan Metode Fuzzy," *JIPI (Jurnal Ilm. Penelit. dan Pembelajaran Inform.*, vol. 8, no. 4, pp. 1439–1450, 2023, doi: 10.29100/jipi.v8i4.4763.

[14] M. Butt, K., Arif, M., & Rafiq, "Assessing university students' satisfaction with web-based

library services based on SERVQUAL model: A case of a Pakistani University," *Libri*, vol. 73, no. 2, pp. 153–165, 2023.

[15] T. S. A. M. Fiqri and A. Alfarisy, "Evaluasi Kualitas Learning Management System berdasarkan ISO 25010 pada SMK Muhammadiyah 1 Palembang," *Explor. J. Sist. Inf. dan Telemat*, vol. 14, no. 1, p. 78, 2023, doi: 10.36448/jsit.v14i1.3116.

Matrix: Jurnal Manajemen Teknologi dan Informatika
Volume 15 Issue 1 Year 2025 Pages 40-49
DOI: http://dx.doi.org/10.31940/matrix.v15i1.40-49
URL: http://ojs2.pnb.ac.id/index.php/matrix

Lightweight CNN with wavelet-attention for fingerprint liveness detection

I Gede Teguh Satya Dharma [1]*, Ni Made Ayu Juli Astari [2]

[1,2] *Information Technology Department, ITB STIKOM Bali, Indonesia*

*Corresponding Author: *teguh@stikom-bali.ac.id*

Abstract: Fingerprint authentication has been extensively employed as a biometric method in diverse applications, including smartphones and embedded systems. Despite its advantages, this technology is susceptible to spoofing attacks using materials such as gelatin, posing a significant security risk. Numerous solutions have been proposed, but deep learning-based approaches often face challenges due to their large model sizes, limiting deployment in resource-constrained environments. To address this issue, we developed a lightweight and efficient fingerprint liveness detection model by integrating wavelet-attention with inverted-bottleneck convolution. The proposed method balances computational efficiency with high accuracy, enabling its practical implementation on low-resource devices. The model was designed with only 874,000 parameters and a memory footprint of 4 MB, representing a significant reduction in size compared to conventional deep learning models. The use of wavelet-attention enhances feature extraction by focusing on multi-scale spatial details crucial for distinguishing live and spoof fingerprints. Extensive experiments were conducted on the LivDet dataset and a custom dataset, encompassing fingerprints captured from multiple sensors. The results demonstrated robust performance, achieving an average classification error (ACE) of 2.27 across various sensors, which is competitive with state-of-the-art methods. Additionally, the model exhibited consistent performance in scenarios with limited computational resources, highlighting its efficiency and scalability. These findings suggest that the proposed approach is a viable solution for enhancing the reliability of fingerprint liveness detection, particularly in applications requiring lightweight and resource-efficient models.

Keywords: convolutional neural network, fingerprint liveness detection, lightweight architecture, wavelet-attention

History Article: Submitted 3 February 2025 | Revised 26 March 2025 | Accepted 19 April 2025

How to Cite: I. G. T. S. Dharma and N. M. A. J. Astari, "Lightweight CNN with wavelet-attention for fingerprint liveness detection", *Matrix : Jurnal Manajemen Teknologi dan Informatika*, vol. 15, no. 1, pp. 40–49, 2025. doi.org/10.31940/matrix.v15i1.40-49.

Introduction

Fingerprint recognition has emerged as a widely adopted authentication method in contemporary systems. This biometric approach has been integrated into numerous applications, ranging from smartphone devices to laptop computers, as a primary authentication mechanism [1]. The preference for fingerprint-based biometric security systems over alternative biological components—such as electrocardiograms, electroencephalograms, iris scans, and facial recognition—can be attributed to its comparatively straightforward authentication process. The widespread adoption of fingerprint authentication in digital systems has precipitated significant security and privacy concerns within the field of biometrics.

As with other authentication mechanisms, fingerprint-based systems introduce unique vulnerabilities to the security landscape. Of particular concern is the threat of fingerprint spoofing. Empirical studies have demonstrated that the success rate of fingerprint spoofing attacks can range from 68% to 100% [2]. These artificial fingerprints are typically fabricated using various material combinations, including gelatin and plastic molds [3]. The high efficacy of these forgery techniques underscores the critical need for advanced intelligent systems capable of robust liveness detection and fingerprint authenticity verification. There are already so many fingerprint liveness detection exist, ranging from a traditional digital image processing method to the use of deep learning.

The study presented in [4] conducts a comprehensive comparison of several texture feature descriptors, including Binarized Statistical Image Features (BSIF), Local Phase Quantization (LPQ), Weber Local Descriptor (WLD), Local Contrast Phase Descriptor (LCPD), and Rotation Invariant Co-occurrence among adjacent Local Binary Patterns (RicLBP). The findings indicate that the combination of LCPD and WLD enhances the effectiveness of fingerprint liveness detection. Meanwhile, other studies [5], [6], [7] and [8] have explored the synergy between fingerprint pore features, ridges and texture descriptors, demonstrating that integrating these complementary features can further boost the accuracy and reliability of liveness detection systems. Despite this promising approach, the performance of handcrafted features falls short compared to deep learning methods due to their lack of adaptability [9]. One of the first model to employ deep learning techniques in this context was introduced by [10], utilizing pre-trained convolutional neural networks (CNNs) to extract both CNN features and spatial features. The research is then followed by [11] and [12] where a ResNet architecture was combined with Transformer elements to enhance selectivity. By employing 830,000 parameters and multi-head attention layers, LFLDNet effectively extracts crucial information from fingerprint images.

However, while these deep learning approaches, including LFLDNet, demonstrate significant improvements in feature extraction and selectivity, they often come with substantial computational costs. The complexity of models like ResNet combined with Transformers requires considerable processing power and memory, making them less suitable for resource-constrained environments. This trade-off between performance and efficiency remains a challenge in the application of deep learning for liveness detection systems. One model that caught our attention for its lightweight nature is FLDNet [13]. FLDNet, a dense model, exhibits a remarkably low misclassification rate of just 2%, coupled with a relatively small number of parameters. Previous studies have demonstrated that incorporating attention layers in deep learning models can significantly reduce the parameter count without sacrificing performance [9], [10]. However, dense models like FLDNet face limitations compared to alternatives such as wavelet-attention and convolutional models. Dense models generally struggle with efficiently capturing spatial hierarchies and multi-scale features, which are critical for robust liveness detection. In contrast, wavelet-attention, which integrates wavelet transforms with attention mechanisms, allows the model to more effectively extract critical features by considering spatial scale variations, while convolutional layers excel at learning localized patterns.

To produce a lightweight and effective model, we employ an attention mechanism inspired by [11], utilizing wavelet-attention due to its proven superiority over conventional attention methods. This approach enables more efficient capture of fine details in image data while comprehensively addressing spatial scale variations. Additionally, we incorporate channel-wise convolution to further reduce the number of parameters without sacrificing the model's ability to extract critical features. By combining wavelet-attention with this convolutional technique, our model achieves enhanced efficiency and accuracy in liveness detection.

Methodology

Architectural Design

This research aims to develop a lightweight fingerprint liveness detection model with a compact architecture and high accuracy, specifically optimized for deployment in resource-constrained environments. The study was divided into three key phases: Our proposed model extends the MobileNetV2 architecture [14], incorporating a novel attention mechanism. Leveraging the Inverted Bottleneck block from MobileNetV2, we maintain a lightweight model suitable for resource-constrained environments. The comprehensive architecture is illustrated in Figure 1. The model is structured into three distinct stages, each designated for specific tasks. The initial stage, termed the "feet," processes high-level features from the input image, efficiently extracting information and rapidly reducing the image size.

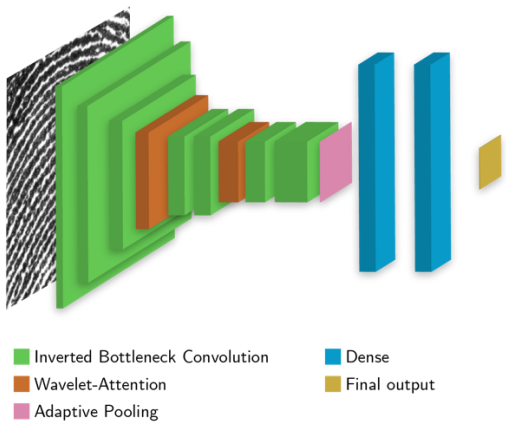

Figure 1. The proposed model architecture

The subsequent stage, referred to as "the body", focuses on intermediate feature extraction and transformation. This stage employs the Wavelet-Attention mechanism, enhancing the model's ability to capture and refine intricate details. By leveraging wavelet transforms, the body stage effectively balances computational efficiency with feature richness, ensuring robust performance across diverse input variations. This design allows for detailed feature representation while maintaining the model's overall efficiency. The final stage, termed "the head," is dedicated to final feature aggregation and classification.

This stage consists of two Inverted Bottleneck layers, which further refine the features extracted from the previous stages. Following these layers, an adaptive pooling layer is employed to ensure a consistent output size, regardless of the input dimensions. The output is then flattened and passed through a linear layer, which performs the final classification. This structured approach ensures that the model effectively integrates features at multiple scales, culminating in a robust and accurate classification output. The overall detail of the proposed architecture can be seen through Figure 1 and Table 1.

Table 1. Proposed model layer detail

Stage	Layer	Kernel Size/Expansion Factor/Stride	Output Shape (W, H, C)
Feet	Inverted Bottleneck	$(1 \times 1), (3 \times 3)/1/2$	(112, 112, 32)
	Inverted Bottleneck	$(1 \times 1), (3 \times 3)/1/2$	(56, 56, 64)
	Inverted Bottleneck	$(1 \times 1), (3 \times 3)/1/2$	(28, 28, 72)
Body	Inverted Bottleneck	$(1 \times 1), (3 \times 3)/1/2$	(28, 28, 72)
	Wavelet-Attention	-	(28, 28, 72)
	Inverted Bottleneck	$(1 \times 1), (3 \times 3)/1/2$	(14, 14, 92)
	Wavelet-Attention	-	(14, 14, 92)
Head	Inverted Bottleneck	$(1 \times 1), (3 \times 3)/1/2$	(14, 14, 216)
	Inverted Bottleneck	$(1 \times 1), (3 \times 3)/1/2$	(14, 14, 216)
	Adaptive Average Pool	-	(1, 1, 216)
	Flatten	-	(32, 16)
	Linear	1	(32, 1)

Wavelet-Attention Mechanism

The wavelet-attention mechanism employed in this model draws inspiration from [15]. Consider an image I with dimensions $M \times N$. As I represents a digital signal, it can be decomposed into multiple sub-bands wavelets w using the discrete wavelet transform (DWT) with a specific wavelet family γ, as expressed in Equation (1). This decomposition yields in a series of sub-band coefficients that encapsulate various frequency components of the original image. Specifically, w_{ll} represents approximate image details, meanwhile w_{lh}, w_{hl} and w_{hh} represent image details.

The novelty of our research lies in our distinctive utilization of these sub-bands. We concatenate each of these wavelets to construct a comprehensive feature map.

$$DWT_{\gamma}(I) = \{w_{ll}, w_{lh}, w_{hl}, w_{hh}\} \tag{1}$$

$$I_m = \sum_{i=0}^{4} c_i w_i \tag{2}$$

$$O = I \bowtie \left(\sigma(I_m)\right) \tag{3}$$

Unlike [15], which discards the w_{hh} sub-band due to the belief that it contains only noise, our approach leverages a weighted sum of all sub-bands, as expressed in Equation (2). In Equation (2), I_m represents the resulting feature map, w_i denotes the sub-band coefficients and c_i are the corresponding weights assigned to each sub-band. This method ensures that our model effectively harnesses the complete frequency information, thereby enhancing feature extraction and overall performance. Sigmoid activation function is then applied to the weighted sum and since the concatenation process of feature maps produced a downsampled vector, we perform bilinear interpolation to upsample the vector back to its original size and perform multiplication between image I and activated feature map $I \bowtie (\sigma(I_m))$ as expressed in Equation (3). Overall, the complete process of wavelet-attention blocks is illustrated in Figure 2.

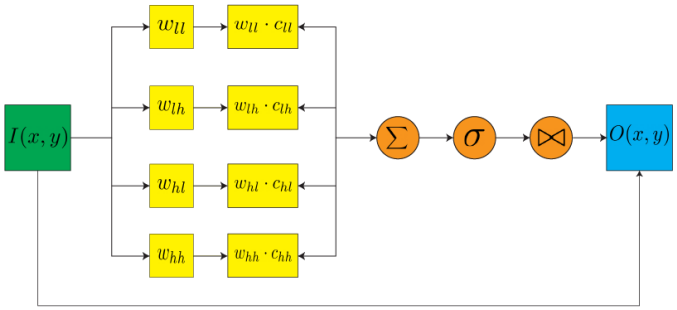

Figure 2. Visualization of wavelet-attention mechanism

By incorporating this attention mechanism, we enhance the network's ability to adaptively weight different regions and scales of the input, leading to improved feature representation and ultimately better performance in various computer vision tasks. The bilinear interpolation step ensures that the attention map aligns properly with the original input dimensions, maintaining spatial coherence throughout the network. This approach not only improves the model's efficiency in processing complex visual information but also contributes to its interpretability, as the attention maps can be visualized to gain insights into the network's decision-making process.

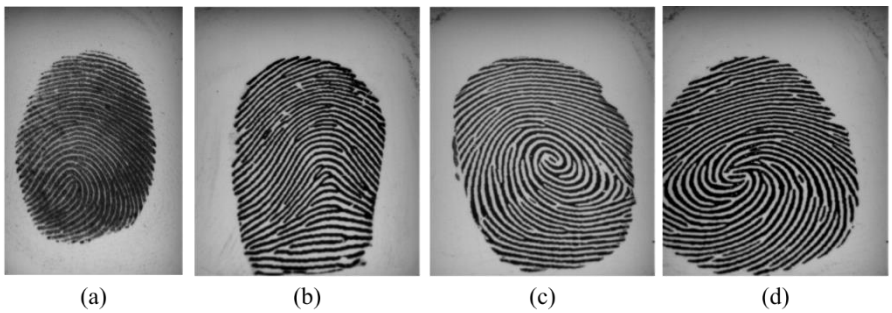

Figure 3. Representative samples from the dataset. From left to right: (a) Real fingerprint, and (b), (c), (d) are spoof fingerprints created using different materials: wood glue, latex, and gelatin, respectively.

Dataset

The dataset utilized in this study is derived from the LivDet (Liveness Detection) Fingerprint Competitions held in 2009 [16], 2011 [17], 2013 [18] and 2015 [19]. This comprehensive dataset encompasses two primary categories: "genuine" and "fake" fingerprints. The "fake" fingerprint samples were obtained using various sensor technologies, which evolved and improved with each competition year, providing a diverse and challenging set of spoof attempts to analyze. The dataset's composition reflects the advancement in both fingerprint acquisition technologies and spoofing techniques over the years.

The "genuine" category consists of real fingerprints collected under controlled conditions, while the "fake" category includes a wide array of artificial fingerprints created using materials such as gelatin, silicone, and play-doh, among others. Figure 3 illustrates representative samples from the dataset, including one genuine fingerprint and several fake samples produced using different spoofing materials. Table 1 provides a detailed breakdown of the total number of genuine and fake fingerprint samples used in this study. It is important to note that the initial dimensions of the fingerprint images vary significantly across the dataset. This variation is due to the different sensors used in each competition year and the specific acquisition protocols followed. The 2009 competition used 3 different sensors, while both 2011 and 2013 used 4 sensors each, resulting in a diverse dataset with varying image sizes and characteristics. The distribution of the fingerprint samples can be seen in Table 2.

Table 2. Distribution of fingerprint samples in LivDet competitions (2009-2015)

Year	Total Genuine Samples	Total Fake Samples	Total Samples
2009	5,493	550	10,993
2011	8,012	7,835	15,847
2013	8,874	8,629	17,503
2015	13,459	15,968	29,427

Implementation Details

The model was trained for a minimum of 10 epochs using the Adam optimizer with AMSGrad. The initial learning rate was set to 1×10^{-4} with mini-batches of 32 images. A *ReduceLROnPlateau* scheduler was implemented, reducing the learning rate by a factor of 0.1 after 2 epochs without improvement in validation performance.Training was conducted on two hardware configurations: a Google Colab environment with NVIDIA V100 GPU and a Lenovo X270 laptop (Intel Core i5-7200U, 8GB RAM). This dual-platform training approach was employed to assess the model's performance under varying computational constraints, relevant for both cloud-based and edge computing scenarios in computer vision applications.

For performance evaluation, we adopt common metrics used in fingerprint liveness detection, including FERRLive, FERRFake and Average Classification Error (ACE) [19]. FERRLive is defined as the percentage of live fingerprints that are incorrectly classified as fake, while FERRFake denotes the percentage of fake fingerprints misclassified as live. The ACE value reflects the average of these two errors, offering a balanced measure of overall classification performance. Let $n(y_l)$ and $n(y_f)$ denote the number of ground-truth live and fake fingerprint samples respectively. Let $n(\hat{y}_l)$ and $n(\hat{y}_f)$ be the number of fake samples misclassified as live. The evaluation metrics are computed as follows:

$$FERR_{live} = \frac{n(\hat{y}_l \neq y_l)}{n(y_l)} \times 100\% \quad (4)$$

$$FERR_{fake} = \frac{n(\hat{y}_f \neq y_f)}{n(y_f)} \times 100\% \quad (5)$$

$$ACE = \frac{FERR_{live} + FERR_{fake}}{2} \times 100\% \quad (6)$$

It is important to note that all reported error rates are expressed in percentage format (0–100%), not as normalized fractions between 0 and 1. Therefore, ACE values greater than 1 are valid and represent percentage error, not normalized error.

Results and Discussions

Results

The experimental results underscore that our proposed model, which incorporates a custom wavelet-attention mechanism, achieves performance competitive with state-of-the-art methods. As detailed in Table 3, the model's performance varies across different sensor types and data years. Notably, it attains an ACE of 1.716% with the CrossMatch sensor, demonstrating its effectiveness in this context, while a higher ACE of 2.198% is observed with the DigitalPersona sensor, suggesting areas for further optimization.

Table 3. Performance comparison of our model compared to existing methods on LivDet 2015 dataset

Method	ACE's Score on LivDet2015 Test Dataset (%)				
	Biometrika	**CrossMatch**	**Digital Persona**	**GreenBit**	**Average**
DRN	6.24	3.46	6.8	4.77	5.32
fPADNet	4.1	0.3	8.5	1.4	3.58
FLDNet	2.34	1.54	2.58	0.56	1.76
Our model	**2.55**	**1.71**	**2.98**	**2.47**	**2.27**

Despite an average ACE of 2.274%, which slightly exceeds the state-of-the-art benchmark of 1.38, the efficiency of the proposed model remains noteworthy. With only 874,000 parameters and a total size of 4 MB, the model effectively balances performance and computational efficiency. However, the observed ACE can largely be attributed to architectural choices made to achieve such lightweight efficiency. Speicifically, the use of single-level wavelet decomposition and static weighting significantly simplifies the network and reduce computational complexity. It also limits the model's ability to extract complex, multi-scale features essential for robust fingerprint liveness detection. This trade-off is consistent with recent findings in the literature. For instance, research done by [20] demonstrated that lightweight architecture relying on simplified decomposition techniques often struggle to capture fine-grained details, leading to higher error rates.

Similarly, [21] reported that while static weighting schemes provide computational advantages, they frequently hinder a model's adaptability to the inherent variability in real-world data. Moreover, the performance discrepancies observed between CrossMatch and DigitalPersona sensors highlight the challenges posed by sensor heterogeneity, a factor that [22] found to significantly impact detection outcomes in multi-sensor systems.In resource-constrained scenarios, an ACE value of 2.274 remains within an acceptable range, aligning with trends observed in lightweight architectures optimized for real-time applications. Future research should focus on incorporating advanced multi-level decomposition techniques and adaptive weighting strategies to enhance the model's representational capacity while preserving its computational efficiency.

While existing methods have largely focused on traditional convolutional architectures or transformer-based models, the proposed wavelet-attention framework offers a promising direction for enhancing both feature extraction and computational efficiency. This pioneering approach lays the foundation for future advancements in biometric security, encouraging further exploration into hybrid architectures that leverage wavelet-based transformations alongside dynamic attention mechanisms to improve adaptability and robustness in real-world applications.

Ablation Studies

We conducted an ablation study to assess the efficacy of our proposed wavelet-attention layer by comparing it to a baseline model using standard pooling operations. The experimental results, summarized in Figure 4, provide strong empirical evidence demonstrating the superiority

of wavelet-attention across multiple fingerprint datasets. Specifically, our model achieved an error rate of 2.550 on the Biometrika dataset, compared to 3.025 for the baseline model, reflecting a 15.7% reduction. Similar improvements were observed for the CrossMatch dataset (1.710 vs. 2.227, 23.2% reduction), the Digital Persona dataset (2.980 vs. 4.495, 33.7% reduction), and the GreenBit dataset (2.470 vs. 3.751, 34.2% reduction). These consistent performance gains across diverse fingerprint sensors underscore the robustness and generalizability of our approach.

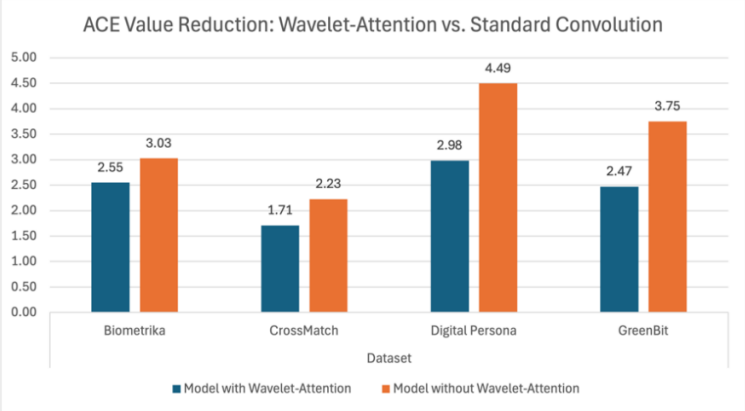

Figure 4. ACE Score comparisons between proposed wavelet-attention convolution and standard convolution

The justification for these improvements lies in the ability of the wavelet-attention layer to efficiently extract and retain both global and local spatial information while mitigating unnecessary redundancy. Unlike conventional convolutional layers, which apply fixed-size filters across the image and tend to lose high-frequency details, wavelet-based transformations decompose input features into multiple frequency components, preserving fine-grained structures crucial for distinguishing live and spoofed fingerprints.

Furthermore, the integration of an attention mechanism amplifies these advantages by dynamically weighting relevant features at multiple scales, ensuring that key discriminatory patterns are emphasized while less informative regions are suppressed. This combination of wavelet decomposition and attention enables our model to capture both long-range dependencies and fine-scale details, enhancing its capacity to generalize across different sensor types. Additionally, recent studies [23] have demonstrated that adaptive wavelet pooling strategies improve classification accuracy by maintaining critical structural information while reducing computational overhead, further supporting the observed reductions in ACE values in our experiments.

Notably, the most significant performance gains were observed for the Digital Persona (33.7%) and GreenBit (34.2%) datasets, both of which have historically posed challenges due to their susceptibility to spoofing artifacts. This suggests that wavelet-attention is particularly effective in fingerprint authentication tasks where fine-scale textural variations play a crucial role in differentiating real from fake prints. Given the absence of prior work explicitly integrating wavelet-based processing with attention mechanisms for fingerprint liveness detection, our approach establishes a novel and promising direction for future research in biometric security. These findings highlight the potential of wavelet-attention as a fundamental building block for more robust and efficient fingerprint recognition systems, paving the way for further advancements in multi-scale feature learning and adaptive deep learning architectures.

Discussions

The results demonstrate that the incorporation of a custom wavelet-attention mechanism into our model effectively balances performance with computational efficiency. Although our model's average ACE of 2.27 is slightly higher than the benchmark of 1.38, it consistently performs well across a variety of sensor types, particularly achieving an ACE of 1.716 with the CrossMatch sensor. This performance, coupled with the model's compact architecture—boasting only 874,000

parameters and a 4 MB footprint—highlights its suitability for deployment in resource-constrained environments. In contrast to larger, more computationally intensive state-of-the-art models, our approach provides a compelling trade-off between accuracy and efficiency, a critical consideration for real-world applications.

Nonetheless, the discussion of our findings also brings to light several limitations inherent in the current design. The use of only a level 1 wavelet decomposition, while effective for reducing computational complexity, may restrict the model's ability to capture finer-scale features, which could be essential for handling more complex or variable biometric data. Additionally, the reliance on static weights for the wavelet components—implemented to avoid overfitting—limits the adaptability of the model. Experiments with learnable weights resulted in rapid overfitting, suggesting that a more nuanced approach to dynamic weighting is necessary to enhance generalization without compromising the model's stability.

Our model has a compact raw size of only 4.00 MB, without the application of any compression techniques such as pruning, quantization, or weight sharing. This baseline footprint demonstrates the efficiency of our architecture by design, and serves as a strong starting point for further optimization. Compared to existing models such as FLDNet (~1.9 MB, 0.48M parameters) and fPADNet (~1.2 MB, 308K parameters), our model offers a balanced trade-off between size and performance, particularly in terms of generalization across multiple sensors. Given that our 4 MB size is achieved without any post-training compression, there is significant room for further reduction if needed, making it highly practical for real-world applications with strict resource constraints. This positions our approach as not only accurate and robust, but also scalable and deployment-ready from the outset.

Looking forward, these observations provide a clear pathway for future improvements. Exploring multi-level decomposition techniques could enable the model to extract richer, hierarchical features, thereby potentially reducing the performance gap with the state-of-the-art. Moreover, developing adaptive weighting mechanisms that strike a balance between flexibility and regularization may mitigate the overfitting issues encountered during initial experiments. Such refinements could further bolster the model's robustness and applicability across diverse biometric datasets, ultimately advancing the field of biometric security by offering solutions that are both effective and computationally efficient.

Conclusion

In this work, we employed and refined the Wavelet-Attention Mechanism specifically for fingerprint liveness detection. Our experiments reveal that incorporating this mechanism leads to substantial performance gains. Evaluated on the LivDet 2015 dataset, our proposed model, which is notably lightweight, achieved an average ACE of 2.27 across all sensor types, ranking as the second-best model among state-of-the-art approaches. This highlights the effectiveness of wavelet-based attention mechanisms in enhancing liveness detection accuracy while maintaining a compact architecture.

Additionally, ablation studies show that our refinements lead to performance improvements ranging from 15.7% to 33.7%, further validating the benefits of our approach. Future work will focus on exploring the use of multilevel wavelet transforms instead of single-level ones to potentially enhance performance further. Another avenue for research includes developing a learnable wavelet family to optimize feature extraction capabilities

Acknowledgments

The authors would like to acknowledge the Kementerian Pendidikan, Kebudayaan, Riset dan Teknologi Republik Indonesia for their financial support of this research through the Hibah Penelitian Dosen Pemula 2024. Their contribution has been crucial in facilitating this work and advancing our research in fingerprint liveness detection.

References

[1] A. A. Abd El-Latif, M. A. Hammad, Y. Maleh, B. B. Gupta, and W. Mazurczyk, *Artificial Intelligence for Biometrics and Cybersecurity Technology and applications* , 1st ed., vol. 1. The Institution of Engineering and Technology, 2023.

[2] M. Chen, C. Yuan, and Y. Lv, "Fingerprint liveness detection approaches: a survey," *Int J Auton Adapt Commun Syst*, vol. 16, no. 6, pp. 564–583, 2023, doi: 10.1504/IJAACS.2023.134830.

[3] S. Agarwal, A. Rattani, and C. R. Chowdary, "A comparative study on handcrafted features v/s deep features for open-set fingerprint liveness detection," *Pattern Recognit Lett*, vol. 147, pp. 34–40, Jul. 2021, doi: 10.1016/j.patrec.2021.03.032.

[4] R. P. Sharma and S. Dey, "A comparative study of handcrafted local texture descriptors for fingerprint liveness detection under real world scenarios," *Multimed Tools Appl*, vol. 80, no. 7, pp. 9993–10012, Mar. 2021, doi: 10.1007/s11042-020-10136-9.

[5] D. Agarwal and A. Bansal, "Fingerprint liveness detection through fusion of pores perspiration and texture features," *Journal of King Saud University - Computer and Information Sciences*, vol. 34, no. 7, pp. 4089–4098, Jul. 2022, doi: 10.1016/j.jksuci.2020.10.003.

[6] C. Yuan, P. Yu, Z. Xia, X. Sun, and Q. M. J. Wu, "FLD-SRC: Fingerprint Liveness Detection for AFIS Based on Spatial Ridges Continuity," *IEEE J Sel Top Signal Process*, vol. 16, no. 4, pp. 817–827, Jun. 2022, doi: 10.1109/JSTSP.2022.3174655.

[7] J. Li, Y. Chen, and E. Zhang, "Comprehensive edge direction descriptor for fingerprint liveness detection," *Signal Process Image Commun*, vol. 102, p. 116603, Mar. 2022, doi: 10.1016/j.image.2021.116603.

[8] R. C. Contreras *et al.*, "A New Multi-Filter Framework for Texture Image Representation Improvement Using Set of Pattern Descriptors to Fingerprint Liveness Detection," *IEEE Access*, vol. 10, pp. 117681–117706, 2022, doi: 10.1109/ACCESS.2022.3218335.

[9] S. Agarwal, A. Rattani, and C. R. Chowdary, "A comparative study on handcrafted features v/s deep features for open-set fingerprint liveness detection," *Pattern Recognit Lett*, vol. 147, pp. 34–40, Jul. 2021, doi: 10.1016/j.patrec.2021.03.032.

[10] Mukul and M. Lal, "Fingerprint Liveness Detection Using Convolutional Neural Network Based Hybrid Model," *NeuroQuantology*, vol. 20, no. 2, pp. 619–633, Feb. 2022.

[11] D. A. Muhtasim, M. I. Pavel, and S. Y. Tan, "A Patch-Based CNN Built on the VGG-16 Architecture for Real-Time Facial Liveness Detection," *Sustainability*, vol. 14, no. 16, p. 10024, Aug. 2022, doi: 10.3390/su141610024.

[12] K. Zhang, S. Huang, E. Liu, and H. Zhao, "LFLDNet: Lightweight Fingerprint Liveness Detection Based on ResNet and Transformer," *Sensors*, vol. 23, no. 15, p. 6854, Aug. 2023, doi: 10.3390/s23156854.

[13] Y. Zhang, S. Pan, X. Zhan, Z. Li, M. Gao, and C. Gao, "FLDNet: Light Dense CNN for Fingerprint Liveness Detection," *IEEE Access*, vol. 8, pp. 84141–84152, 2020, doi: 10.1109/ACCESS.2020.2990909.

[14] M. Sandler, A. Howard, M. Zhu, A. Zhmoginov, and L.-C. Chen, "MobileNetV2: Inverted Residuals and Linear Bottlenecks," Jan. 2018, [Online]. Available: http://arxiv.org/abs/1801.04381.

[15] X. Zhao, "Wavelet-Attention CNN for Image Classification," 2022.

[16] G. L. Marcialis *et al.*, "First International Fingerprint Liveness Detection Competition—LivDet 2009," 2009, pp. 12–23. doi: 10.1007/978-3-642-04146-4_4.

[17] D. Yambay, L. Ghiani, P. Denti, G. L. Marcialis, F. Roli, and S. Schuckers, "LivDet 2011 — Fingerprint liveness detection competition 2011," in *2012 5th IAPR International Conference on Biometrics (ICB)*, IEEE, Mar. 2012, pp. 208–215. doi: 10.1109/ICB.2012.6199810.

[18] L. Ghiani *et al.*, "LivDet 2013 Fingerprint Liveness Detection Competition 2013," in *2013 International Conference on Biometrics (ICB)*, IEEE, Jun. 2013, pp. 1–6. doi: 10.1109/ICB.2013.6613027.

[19] V. Mura, L. Ghiani, G. L. Marcialis, F. Roli, D. A. Yambay, and S. A. Schuckers, "LivDet 2015 fingerprint liveness detection competition 2015," in *2015 IEEE 7th International Conference on Biometrics Theory, Applications and Systems (BTAS)*, IEEE, Sep. 2015, pp. 1–6. doi: 10.1109/BTAS.2015.7358776.

[20] K. Zhang, S. Huang, E. Liu, and H. Zhao, "LFLDNet: Lightweight Fingerprint Liveness Detection Based on ResNet and Transformer," *Sensors*, vol. 23, no. 15, Aug. 2023, doi: 10.3390/s23156854.

[21] J. Chen, C. Yuan, C. Cui, Z. Xia, X. Sun, and T. Akilan, "A Lightweight Convolutional Neural Network with Representation Self-challenge for Fingerprint Liveness Detection," *Computers, Materials and Continua*, vol. 73, no. 1, pp. 719–733, 2022, doi: 10.32604/cmc.2022.027984.

[22] R. Kiefer and A. Patel, "A Comprehensive Survey on Fingerprint Liveness Detection Algorithms by Database and Scanner Model," in *Advances in Security, Networks, and Internet of Things* , 2021, pp. 39–51. doi: 10.1007/978-3-030-71017-0_4.

[23] J. Sun *et al.*, "Cascade wavelet transform based convolutional neural networks with application to image classification," *Neurocomputing*, vol. 514, pp. 285–295, Dec. 2022, doi: 10.1016/j.neucom.2022.09.149.

POLITEKNIK NEGERI BALI

9 772580 563008

Redaksi Jurnal Matrix
Gedung P3M, Politeknik Negeri Bali
Bukit Jimbaran, PO BOX 1064 Tuban, Badung, Bali.
Phone: +62 361 701981, Fax: +62 361 701128
e-mail: p3mpoltekbali@pnb.ac.id
https://ojs2.pnb.ac.id/index.php/MATRIX